

# **ESTABLISHING A RISK PROFILE FOR METAL NEUROTOXICITY AND NEURODEGENERATION IN KEY SOUTH AFRICAN MINING:**

**A local water quality assessment**

Report to the  
**Water Research Commission**

by

**B Loos, S Cogill and A Mangali**  
Department of Physiological Sciences  
Stellenbosch University

**WRC Report No. 3077/1/23**  
**ISBN 978-0-6392-0408-6**

**May 2023**



**Obtainable from**

Water Research Commission  
Bloukrans Building, 2<sup>nd</sup> Floor  
Lynnwood Bridge Office Park  
4 Daventry Road  
Lynnwood Manor  
PRETORIA

[orders@wrc.org.za](mailto:orders@wrc.org.za) or download from [www.wrc.org.za](http://www.wrc.org.za)

The publication of this report emanates from a project entitled, *Establishing a risk profile for metal neurotoxicity and neurodegeneration in key South African mining communities – a local water quality assessment* (WRC Project No. C2021/2023-00518)

**DISCLAIMER**

This report has been reviewed by the Water Research Commission (WRC) and approved for publication. Approval does not signify that the contents necessarily reflect the views and policies of the WRC, nor does mention of trade names or commercial products constitute endorsement or recommendation for use.

## EXECUTIVE SUMMARY

---

Alzheimer's disease (AD) is the most prevalent neurodegenerative disorder that typically presents with the progressive loss of cognitive function. Albeit major efforts in research conduct worldwide, no disease modifying treatment exists. Most significant, in terms of quality of life as well as health care costs, is the development of dementia, with AD accounting for nearly 50 million of all dementia cases worldwide. The prevalence is increasing rapidly, and it is estimated that the number of AD patients globally will rise to 152 million by 2050. It is predicted that low and medium income countries will be especially adversely affected, putting South Africa at a greater risk. Importantly, poor water quality has been associated with the risk for developing neurodegenerative disease, particularly due to metal neurotoxicity, facilitated by heightened levels of copper, manganese, cadmium and iron. High mining activity contributes to this risk by impacting water quality in regions of intense mining, contributing to a vulnerable water scenario in terms of required fresh water access. However, to what extent local water quality may indeed impact markers for neurotoxicity and increase the risk for developing neurodegenerative disease in South Africa is unknown.

The following were the aims of the project:

1. By using IC-PMS analysis techniques, profile the metal concentration of water samples collected from 2 major geographical mine regions associated with iron, manganese, copper and cadmium.
2. Create an *in vitro* environment reflective of results gathered through aim 1, and subsequently assess neuronal cells for specific markers for autophagy, mitochondrial function and lysosome function, associated with neurotoxicity.
3. By using an APP-overexpression model associated with Alzheimer's disease, measure the amyloidogenic properties, including A-beta generation, using western blotting, transfections using an autophagy flux construct and life cell imaging, linked to quantitative pool size analysis.
4. By pre-treating cells with resveratrol prior to exposure to metal-contaminated to assess the potential protective effects of autophagy enhancements by measuring and quantifying neuronal toxicity and A-beta clearance.

The findings from this study have shown that Cd and Cu have the potential to further exacerbate neurotoxicity in a pre-existing neurodegenerative environment in the context of APP over-expression. Thus, more attention may have to be paid to preventing the exposure to these specific heavy metals. Moreover, our findings show that surface and river water in the Northern Cape region are a concern, which requires further attention. These findings are of particular importance due to the communities typically exposed to the surface water, either through dermal contact or, given the poor sanitation and water shortage in the region, water ingestion.

Taken together, this research highlights that, although municipal water sources in the two respective mining regions are safe and within the regulatory limits, the surface water poses a substantial risk. Moreover, our results reveal that also borehole water may pose a risk, as indicated by the high arsenic levels in one sampling region in the Limpopo area. Indeed, the suspected metals cadmium, copper and manganese appear to have, molecularly, major detrimental effects. Iron, manganese and copper, but also aluminium concentrations are above respective limits in the surface and river waters, which poses risk for the environment and the community in close proximity to these regions.

The findings from this study can be used to inform the development of guideline values (maximum allowable limits for exposure) for these metals, treatment methods for heavy metal removal in water and as well as inform possible departure for a conversation for other heavy-mining countries to take similar precautions to protect those exposed to heavy metals. In South Africa, this is the first study to assess metal toxicity in the context of neurodegeneration within mining populations. These findings are of particular importance due to the high concentration of copper (mines) and gold mines (mines, of which cadmium is a by-product) found in South Africa. Further action in this context, such as *in vivo* studies, social and corporate activity and prophylactic interventions are recommended for further work.

## ACKNOWLEDGEMENTS

The authors would like to thank the Reference Group of the WRC Project for the assistance and the constructive discussions during the duration of the project. These have been highly informative. The authors wish to thank the WRC for funding this work (Project No. C2021/2023-000518).

<b>Research group members</b>	<b>Affiliation</b>
Wolfaardt, GM, Prof	Stellenbosch University
Botes, M, Dr	Stellenbosch University
Sinnead Cogill	Stellenbosch University
Asandile Mangali	Stellenbosch University
Ben Loos, Prof	Stellenbosch University
<b>Reference Group</b>	<b>Affiliation</b>
Marlene Fourie INFOTOX	INFOTOX
Natasha Sanabria	NHLS, NIOH
Curtis, Christopher	University of Johannesburg
Bettina Genthe	CSIR
Jabulani Gumbo	University of Venda
Charmaine Khanyile	WRC
Nonhlanhla Kalebaila	WRC
<b>Others</b>	
Dr Tando Maduna	Stellenbosch University
Dr Andre du Toit	Stellenbosch University

# CONTENTS

<b>EXECUTIVE SUMMARY</b> .....	<b>iii</b>
<b>ACKNOWLEDGEMENTS</b> .....	<b>iv</b>
<b>CONTENTS</b> .....	<b>v</b>
<b>LIST OF FIGURES</b> .....	<b>vii</b>
<b>LIST OF TABLES</b> .....	<b>ix</b>
<b>ACRONYMS &amp; ABBREVIATIONS</b> .....	<b>x</b>
<b>GLOSSARY</b> .....	<b>xi</b>
<b>CHAPTER 1: BACKGROUND</b> .....	<b>1</b>
1.1 INTRODUCTION .....	1
1.2 RATIONALE FOR THE STUDY .....	2
1.3 PROJECT AIMS AND OBJECTIVES .....	3
1.4 SCOPE AND LIMITATIONS .....	3
<b>CHAPTER 2: ENVIRONMENTAL EXPOSURE TO METALS AND THE DEVELOPMENT OF NEUROGENERATIVE DISEASES</b> .....	<b>4</b>
2.1 INTRODUCTION .....	4
2.2 INTERACTIONS BETWEEN HEAVY METALS, THE BLOOD BARRIER AND GASTROINTESTINAL TRACT .....	6
2.3 ROLE OF HEAVY METALS IN NEURODEGENERATION .....	7
2.3.1 Copper .....	7
2.3.2 Cadmium .....	12
2.3.3 Manganese .....	15
2.3.4 Arsenic .....	19
2.3.5 Iron .....	21
<b>CHAPTER 3: STUDY DESIGN AND METHODS</b> .....	<b>24</b>
3.1 INTRODUCTION .....	24
3.2 SAMPLING AND SAMPLE ANALYSIS .....	24
3.2.1 Study sites and water sample collection .....	24
3.2.2 Assessing the possible cytotoxic effect of the respective metal microenvironment .....	25
3.2.2.1 Proposed flow of experiments .....	25
3.2.2.2 EDX analysis .....	26
3.3 RESULTS AND DISCUSSION .....	27
3.3.1 Metal concentration profile of water samples collected .....	27
3.3.2 Health risk assessment .....	28
3.3.3 Assessing the possible cytotoxic effect of the respective metal microenvironment .....	29
3.3.4 Assessing the intracellular uptake of the metals .....	32
3.3.5 Assessing the impact of metal exposure .....	37
3.3.6 Assessing primary cellular stress response .....	38
3.3.7 Assessing the extent of neuronal toxicity due to metal exposure .....	39
3.3.8 Evaluating the role of the lysosomal compartment as part of the cellular stress response .....	39

3.3.9	Assessing the impact of metal exposure on cell viability and proliferation.....	41
<b>CHAPTER 4:</b>	<b>CONCLUSION AND RECOMMENDATIONS.....</b>	<b>43</b>
4.1	CONCLUSIONS.....	43
4.2	RECOMMENDATIONS.....	43
<b>REFERENCES</b>	<b>.....</b>	<b>44</b>

## LIST OF FIGURES

Figure 2.1: The hallmark features of ageing in comparison to ageing with neurodegeneration, which leads to an increase in cognitive decline and disease. The pathways with which the antioxidant resveratrol, interacts with the system is also demonstrated (Bishop et al., 2010 )(created with BioRender.com).....	4
Figure 2.2: The autophagy process. Macroautophagy begins with the formation of a phagophore that following elongation, forms the autophagosome, a double-membraned vesicle capable of sequestering cargo. Upon fusion with a lysosome to form an autolysosome, the sequestered cargo is degraded by acidic hydrolases. The chaperone-mediated autophagy process begins with the specific targeting of proteins to a lysosome via signal peptides and coordinated chaperones (created with BioRender.com). .....	5
Figure 2.3: The various homeostatic roles of copper inside the cell. With superoxide dismutase (SOD), copper is transported to the mitochondria and through the metallochaperone COX17, is used to ensure cytochrome c oxidase stability. The protein ATX1 transports copper ions to the nucleus for gene expression and to the Golgi body to assist in the transport of ions. Cuproenzymes also make use of copper components in regulating oxygen transport, redox reactions and cellular metabolism (Lutsenko, 2010)(created with BioRender.com). .....	8
Figure 2.4: The effects of excess copper on the cell. An increase in the Fenton reaction for copper with the additional dysregulation of the copper homeostasis, leads to an increase in unbound ions that are capable of binding to APP, Amyloid- $\beta$ and histone residues. The latter leads to a dysregulation in the functioning of the UPS system, as well as mitochondrial dysfunction and ROS generation. Excess copper is capable of increasing the activity of $\beta$ -secretase, and inhibiting astrocyte functioning and insulin degrading enzyme (IDE) pathway responsible for cleaving A $\beta$ . This leads to a loss of the brains neuroprotective capabilities as well as an increase in protein aggregations, both of which are hallmark features for neurodegenerative disease (Brewer et al., 2010) (Pohanka, 2019)(Opazo et al., 2014)(Hsu et al., 2018)(created with BioRender.com).....	9
Figure 2.5: The various effects of cadmium on the brain and the cells of the brain. An excess of cadmium increases BBB permeability which over time leads to excess cadmium in the brain. This has shown to increase Acetylcholinesterase activity which is a known risk for Alzheimer's disease. Inside the cell, cadmium affects the nucleus by upregulating various genes which code for proteins that are responsible for inflammation and oxidative stress (HMOC1), proteotoxic stress (DNAJB1 and HSPA6), DNA damage (GADD45 $\beta$ ) and markers of neurodegeneration (CHOP and GDF15). Cadmium has also shown to impair lysosomal function which results in autophagosome-lysosomal fusion and blocks autophagy flux. The end-result leads to an increase in ROS and oxidative stress, a decrease in various integral antioxidants. With chronic exposure in the brain through these mechanisms, there is an increased risk for brain cancer and neurodegenerative disease (Carageorgiou et al., 2005)(Forcella et al., 2020)(Polykretis et al., 2019)(Rani et al., 2014)(created with BioRender.com).....	13
Figure 2.6: The dysregulation of excess manganese in the brain. Manganese triggers the release of pro-inflammatory cytokines as well as their mRNA translation resulting in excess inflammation and oxidative stress which ultimately leads to mitochondrial dysfunction and apoptosis. With the increase in circulating manganese is the increase in metal transporters. Autophagy regulators such as TFEB are inhibited leading to the accumulation of neurodegenerative proteins (Dobson et al., 2004)(Zhang et al., 2020)( Martins et al., 2019)(created with BioRender.com). .....	18
Figure 2.7: The neurotoxicity caused by excess arsenic or chronic exposure to arsenic in the brain. Arsenic inhibits the functionality of anti-oxidants and upregulates apoptotic proteins and BACE-1, resulting in an accumulation of neurodegenerative proteins, an increase in oxidative stress and mitochondrial dysfunction. It also inhibits various brain signalling pathways and the development of the cytoskeletal network, accelerating neurotoxicity. Arsenic can also associate with molecules including dopamine, leading to an increase in circulating Lewy bodies. (Abdul et al., 2015)( Prakash et al., 2016)(Thakur et al., 2021)(Tyler & Allan, 2014)(created on BioRender.com). .....	20
Figure 2.8: The pathways in which dysfunction and toxicity due to excess iron, occur in the brain. In homeostatic conditions, iron plays an essential role in oxygen transportation in the bloodstream. However which chronic	

exposure to excess iron, the functions in the brain are dysregulated, leading to cell death through ferroptosis and the accumulation of iron-localising toxic proteins (Ndayisaba et al., 2019)(Thomas et al., 2021)(Anderson & Frazer., 2017) (created on BioRender.com).....22

Figure 3.1: Region of sample collection. A total of 11 samples were taken in the encircled regions of the map.....24

Figure 3.2: Sample collection Northern Cape, including rivers, surface water and municipal water sources.....25

Figure 3.3: Overall scheme of experimental design and set up. ....25

Figure 3.4: Feedback Gravelotte primary school, Sept 2022. ....29

Figure 3.5: A – WST-1 assay conducted using increasing Cd concentrations (12,5 µM, 50 µM, and 75 µM) over 24 hours. B – Microscope image of treated cells at a magnification of 40X, following a 24 hour treatment at a Cadmium concentration of 75 µM.....30

Figure 3.6: A – WST-1 assay conducted using increasing Mn concentrations (12,5 µM, 50 µM, and 75 µM) over 24 hours. B – Microscope image of treated cells at a magnification of 40X, following a 24 hour treatment at a Mn concentration of 500 µM. ....30

Figure 3.7: A – WST-1 assay conducted using increasing Cu concentrations (100 µM, 250 µM, and 500 µM) over 24 hours. B – Microscope image of treated cells at a magnification of 40X, following a 24 hour treatment at a Cu concentration of 500 µM. ....31

Figure 3.8: A – WST-1 assay conducted using increasing Fe concentrations (100 µM, 250 µM, and 500 µM) over 24 hours. B – Microscope image of treated cells at a magnification of 40X, following a 24 hour treatment at a Fe concentration of 500 µM.....31

Figure 3.9: A – WST-1 assay conducted using increasing As concentrations (20-100 µM) over 24 and 48 hours. B – Microscope image of treated cells at a magnification of 40X, following a 24 hour treatment at an As concentration of 20 µM. ....32

Figure 3.10: EDX analysis protocol optimisation, to assess the metal elemental profile in neuronal cells.....33

Figure 3.11: A representative (control) EDX analysis using spot quantification, showing average intracellular uptake of all metals of interest.....34

Figure 3.12: A representative EDX analysis using spot quantification, showing average intracellular uptake of Cd. ....34

Figure 3.13: A representative EDX analysis using spot quantification, showing average intracellular uptake of Mn. ....35

Figure 3.14: A representative EDX analysis using spot quantification, showing average intracellular uptake of As.....35

Figure 3.15: A representative EDX analysis using spot quantification, showing average intracellular uptake of Fe.....36

Figure 3.16: A representative EDX analysis using spot quantification, showing average intracellular uptake of Cu. ....36

Figure 3.17: STEM micrographs of N2a cells following various treatment. A: control cells B: exposure to 500 µM Cu for 24 hrs. C: exposure to 500 µM Fe for 24 hrs. D: exposure to 500 µM Mn for 24 hrs. E: exposure to 75 µM Cd for 24 hrs. F: exposure to 0.528 µM As for 48 hrs. Scale bar: 2-4 µm respectively. ....37

Figure 3.18: Western blot analysis for average LC3-I and LC3-II protein abundance. Representative immunoblots for both proteins as well as β-actin are shown for the following groups in the absence (-) and presence (+) of 400 nM Baf: control, 500 µM Cu, 500 µM Fe, 500 µM Mn, 75 µM Cd and 0.528 µM As. A low- and high-exposure micrograph has been provided so as to better visualise LC3-I. \*p<0.05 vs Control, #p<0.05 vs Con + Baf. n=4 .....38

Figure 3.19: Cell viability in the presence of amyloid-induced toxicity. ....39

Figure 3.20: Fluorescence micrographs indicating the nuclei and lysosomal acidic compartments (LAC) of APP cells for the control experiment. Scale bar represents 10  $\mu\text{m}$ . A minimum total number of 2 fields of view each were acquired for 2 independent experiments. ....39

Figure 3.21: Fluorescence micrographs indicating the nuclei and lysosomal acidic compartments (LAC) of APP cells following 500  $\mu\text{M}$  Cu only treatment over 24 hours and 500  $\mu\text{M}$  Cu with 5 mM butyric acid for 6 hours using 2 mg/ml acridine orange dye. Scale bar represents 10  $\mu\text{m}$ . A minimum total number of 2 fields of view each were acquired for 2 independent experiments. ....40

Figure 3.22: Fluorescence micrographs indicating the nuclei and lysosomal acidic compartments (LAC) of APP cells following 75  $\mu\text{M}$  Cd only treatment over 24 hours and 75  $\mu\text{M}$  Cd with 5 mM butyric acid for 6 hours using 2 mg/ml acridine orange dye. Scale bar represents 10  $\mu\text{m}$ . A minimum total number of 2 fields of view each were acquired for 2 independent experiments. ....40

Figure 3.23: Cell viability analysis and cell count for exposure to all metals.....41

Figure 3.24: Cell viability analysis and cell count after exposure to Fe.....41

Figure 3.25: Assessment of mitochondrial fission and fusion proteins after exposure to all metals of interest. ...42

## LIST OF TABLES

---

Table 1.1: Impact of Gold and Copper mining on water resources (Sedibe et al., 2017). .... 1

Table 3.1: LCPMS analysis of 11 samples collected in the Limpopo region.....27

Table 3.2: LCPMS analysis of samples collected in the Northern Cape.....28

Table 3.3: Health risk and hazard quotient analysis.....28

Table 3.4: Health quotient assessment. ....29

## ACRONYMS & ABBREVIATIONS

---

A $\beta$	Amyloid $\beta$
AChE	acetylcholinesterase
AD	Alzheimer's disease
AMD	acid mine drainage
AMPK	AMP- activated protein kinase
APP	amyloid precursor protein
As	arsenic
ATP	adenosine triphosphate
AV	autophagic vacuole
BA	butyric acid
Baf1A	bafilomycin A1
BBB	blood brain barrier
BCB	blood CSF barrier
CCL	carbon chloride
Cd	cadmium
CNS	central nervous system
CO <sub>2</sub>	carbon dioxide
COX	cyclooxygenase
CSF	cerebral spinal fluid
CTR1	copper transporter-1
Cu	copper
DAT	dopamine transporter
dH <sub>2</sub> O	deionised water
LAMP	lysosome-associated membrane protein
LC3	microtubule-associated protein light chain 3
LIBS	laser-induced breakdown spectroscopy
LRP1	lipoprotein receptor-related protein 1
min	minutes
Mn	manganese
mRNA	messenger RNA
mTOR	mammalian target of rapamycin
NaCl	sodium chloride
NADPH	reduced nicotinamide adenine dinucleotide phosphate
ND	neurodegenerative disease
NFTs	neurofibrillary tangles
NMDA	N-methyl-D-aspartic acid
p62	sequestosome-1
PBS	phosphate-buffered saline
PD	Parkinson's disease
RNA	ribonucleic acid
ROS	reactive oxygen species
Rpm	rotations per minute
RT	room temperature
SEM	scanning electron microscopy
STEM	scanning transmission electron microscopy
TEM	transmission electron microscopy
TFEB	transcription factor EB
THQ	target hazard quotient
UPS	ubiquitin proteasome system
USEPA	United States Environmental Protection Agency
WDS	wavelength dispersive spectroscopy
WHO	World Health Organisation
WST-1	water-soluble tetrazolium

## GLOSSARY

---

**Autophagosome.** Intracellular organelle that engulfs and sequesters proteinaceous cargo.

**Autophagy.** A protein degradation system in cells.

**Lysosome.** Acidic organelle that receives intracellular cargo for degradation.

**Neurodegeneration.** A disease associated with neuronal cell death and impairment of cognitive function.

This page was intentionally left blank

# CHAPTER 1: BACKGROUND

## 1.1 INTRODUCTION

Access to safe drinking water has become a growing concern for the country of South Africa. With a population of approximately 59 million, currently 40% of the people in South Africa occupy rural areas where 19% thereof lack access to a reliable water supply and 33% lack basic sanitation services (Water Access in South Africa, 2017). Due to the lack of infrastructure in these areas, approximately 74% of people are almost entirely dependent on groundwater such as local wells, pumps and surrounding riparian areas (Water Access in South Africa, 2017). The use of shallow, hand-dug wells and deep groundwater sources such as boreholes are therefore very common in South Africa. These sources are also poorly managed due to its often-invisible nature as well as the fact that it usually takes an extended period of time to notice that it has become polluted or contaminated (Edokpayi et al., 2018). Research has already reported high levels of faecal and fluoride contamination in groundwater sources in the Limpopo province of South Africa (Edokpayi et al., 2018).

South Africa's mining sector generates 7.4% of the entire country's Gross Domestic Product (GDP), which is a contribution of approximately R286 billion. The sector also plays an integral role in the employment of the country, with the direct employment of approximately half a million people (Askham & Van der Poll, 2017). Despite the positive role mining plays in South Africa's economy, mining operations contribute to various negative effects to water quality such as uncontrolled discharges, the collapse of control dams, the potential flooding of pits as well as acid mine drainage (AMD) (Table 1.1). AMD is defined as a mine waste water effluent which is mostly generated from coal, copper and gold mining operations. It is characterised by low pH content and high heavy mineral/metal content (Mativenga & Marnewick, 2018).

**Table 1.1: Impact of Gold and Copper mining on water resources (Sedibe et al., 2017).**

Sub-basin	Type of Mining	Water Quality Issues
Ngotwane/Bonwapitse	Other	Acid mine drainage
Motlouse	Base metals	Copper accumulation
Shashe	Gold	Copper accumulation & AMD
Mzingwane	Gold	AMD
Marico	Base metals	Copper accumulation

A major concern for AMD is the fact that the rate that these heavy metals accumulate in the water is estimated to be approximately ten-fold of the rate that it mobilizes from natural cycling (Sedibe et al., 2017). South Africa is also one of the top five producers of gold globally (Askham & Van der Poll, 2017). In 2001, South Africa's Department of Water Affairs and Forestry reported that gold mine waste generates the largest single source of waste and makes up roughly 47% of all mineral wastes produced in South Africa (Sedibe et al., 2017). South Africa also contains approximately 80% of the world's known manganese resources, primarily in the Northern Cape. At present, these manganese mines employ approximately 7000 workers (Dlamini et al., 2020).

The increasing levels of heavy metals in the water of South Africa is posing a serious potential health risk, with the water of surrounding mining regions often associated with the heavy metal pollution of copper, manganese, cadmium (a by-product of gold mining) and iron in particular (Pellacani & Costa, 2018). A study conducted in the vicinity of the old Princess gold mine in Johannesburg reported an increase in heavy metal concentrations in analysed soil samples (Olobatoke & Mathuthu, 2015).

Another study aimed to investigate the extent of heavy metal contamination of the irrigation water, soils and fresh produce grown in the Philippi Cape Town area in the Western Cape of South Africa.

In another study, it was reported that cadmium concentrations in the irrigation water collected exceeded or was at the maximum permissible concentrations of 0.05mg/l in water used for irrigation (Malan et al., 2015). These analyses indicate that heavy metals are already of concern in terms of accumulation and environmental pollution in South Africa. According to the South African National Standards (SANS, 2015), a maximal level of <2000µg/L of copper and <3µg/L of cadmium is allowed to be present in drinking water. A dosage of 0.1 to 0.2 mg/kg of copper relative to body weight is considered toxic, and could lead to Wilson's disease, renal damage, cirrhosis, salivary gland swelling, haemolysis and hepatic necrosis. For cadmium, a small chronic dosage of 10µg/d over 50 years could lead to gastric cramps, vomiting, diarrhoea, coughing, headache, brown urine, hypertension, malignancy, immune disorder and renal failure. Cadmium ingested through heavily contaminated water can also result in immediate severe cadmium poisoning (Sedibe et al., 2017).

Based on World Health Organization statistics, the worldwide occurrence concentration ranges of copper and cadmium in freshwater environments are 0.005-30mg/L and less than 1µg/L respectively (Razak et al., 2021). Moreover, these metals have been associated with neurotoxicity and the progression of neurodegenerative disease. In the study conducted by Myers et al., 468 dust measurements were obtained over the course of 4 years in two manganese mining towns in the Northern Cape of South Africa, with the combined total of approximately 2000 employees working in the two mining companies. Of this, 489 subjects were examined through questionnaire, intravenous blood tests and neurobehavioral tests. It was found that only 10% of the subjects had elevated blood manganese (above the average 12ug/L). Furthermore, the study found no manganese exposure related effects (Myers et al., 2003). A later study conducted by Dlamini et al., however, assessed 187 mine-workers in the Northern Cape and found that in this cohort, parkinsonian signs were common and were associated with cumulative manganese exposure and a poor quality of life. They also found a strong association between the progression of clinical parkinsonism and manganese exposure in the early years of exposure (Dlamini et al., 2020).

Alzheimer's disease (AD) is the most prevalent neurodegenerative disorder that typically presents with the progressive loss of cognitive function. Albeit major efforts in research conduct worldwide, no disease modifying treatment exists. Most significant, in terms of quality of life as well as health care costs, is the development of dementia, with AD accounting for nearly 50 million of all dementia cases worldwide. The prevalence is increasing rapidly, and it is estimated that the number of AD patients globally will rise to 152 million by 2050. It is predicted that low and medium income countries will be especially adversely affected, putting South Africa at a greater risk. Importantly, poor water quality has been associated with the risk for developing neurodegenerative disease, particularly due to metal neurotoxicity, facilitated by heightened levels of copper, manganese, cadmium and iron. High mining activity contributes to this risk by impacting water quality in regions of intense mining, contributing to a vulnerable water scenario in terms of required fresh water access. However, to what extent local water quality may indeed impact markers for neurotoxicity and increase the risk for developing neurodegenerative disease in South Africa is unknown.

## **1.2 RATIONALE FOR THE STUDY**

Molecularly, proteotoxicity is a major hallmark in AD progression, indicating loss of proteostasis. Autophagy, from greek 'self-eating' is an intracellular process used for the degradation of long-lived and abnormal proteins. Autophagy dysfunction has been implicated fundamentally in AD, and major efforts

are under way, to explore precision autophagy control for novel treatment approaches. Importantly, autophagy has been implicated in metal neurotoxicity. However, whether specific chemical water parameters from mining-intense regions impact the autophagy machinery and toxic cargo clearance has not yet been assessed.

### 1.3 PROJECT AIMS AND OBJECTIVES

The following were the aims of the project:

1. By using IC-PMS analysis techniques, profile the metal concentration of water samples collected from 2 major geographical mine regions associated with iron, manganese, copper and cadmium
2. Create an *in vitro* environment reflective of results gathered through aim 1, and subsequently assess neuronal cells for specific markers for autophagy, mitochondrial function and lysosome function, associated with neurotoxicity.
3. By using an APP-overexpression model associated with Alzheimer's disease, measure the amyloidogenic properties, including A-beta generation, using western blotting, transfections using an autophagy flux construct and life cell imaging, linked to quantitative pool size analysis.
4. By pre-treating cells with resveratrol prior to exposure to metal-contaminated to assess the potential protective effects of autophagy enhancements by measuring and quantifying neuronal toxicity and A-beta clearance.

### 1.4 SCOPE AND LIMITATIONS

This work seeks to dissect the role of the above specific metals on the molecular markers that are associated with neurodegenerative disease. The concentrations and the duration of exposure are informed by literature and the here implemented toxicity studies. However, the concentrations are also contextualized, and, where possible (see arsenic) implemented, based on the actual metal concentrations that were determined in the two geographic regions. This very approach indicates also its limitations, being an *in vitro* model system, with the absence of the physiological complexity of metal absorption through the GIT, its presence in the plasma, its ability to cross the blood brain barrier, and finally its local concentration and tissue availability in the immediate neuronal microenvironment in the brain. Hence, this project may be seen as points of departure to

- provide the required awareness to metal neurotoxicity in South African mining regions
- measurable metal concentrations in surface water and drinking water in South African mining regions
- contextualized analysis of metal exposure in a globally acceptable model system to study neurotoxicity
- dissection of molecular hallmarks associated with metal neurotoxicity

The above points of departure are framed by the actual metals that are (globally uniquely) mined in South Africa, and hence provides real context and real application. It is hoped that this work provides a starting point to further our understanding of risk and disease for our local mining communities, as is being done in other mining countries, such as Canada, so as to devise respective interventions to protect the local population residing in the areas assessed in this study.

## CHAPTER 2: ENVIRONMENTAL EXPOSURE TO METALS AND THE DEVELOPMENT OF NEUROGENERATIVE DISEASES

### 2.1 INTRODUCTION

Neurodegeneration is defined as the progressive atrophy and loss of function of neurons. This can be seen in numerous neurodegenerative diseases such as Alzheimer’s disease, Parkinson’s disease and Huntington’s disease, which are characterized by the presence of cytoplasmic and nuclear protein aggregates that result in toxicity and neuronal death (Lumkwana et al., 2017). The primary risk factor for neurodegenerative diseases is ageing. Figure 2-1 demonstrates the various hallmark features of ageing such as DNA damage, mitochondrial dysfunction, telomere shortening and a reduction in autophagy contribute to a gradual cognitive decline over time. These features lay the foundation for an increase in neurodegeneration, when combined with other factors such as genetics and lifestyle (Bishop et al., 2010). An increase in heavy metal accumulation has been linked to neurodegeneration. There is also evidence for the age-related increase in metals such as copper and iron in the brain. For example, the disruption of homeostatic processes and mechanisms involving metals in the brain have been suggested to contribute to sporadic forms of Alzheimer’s disease (Yokel, 2006).

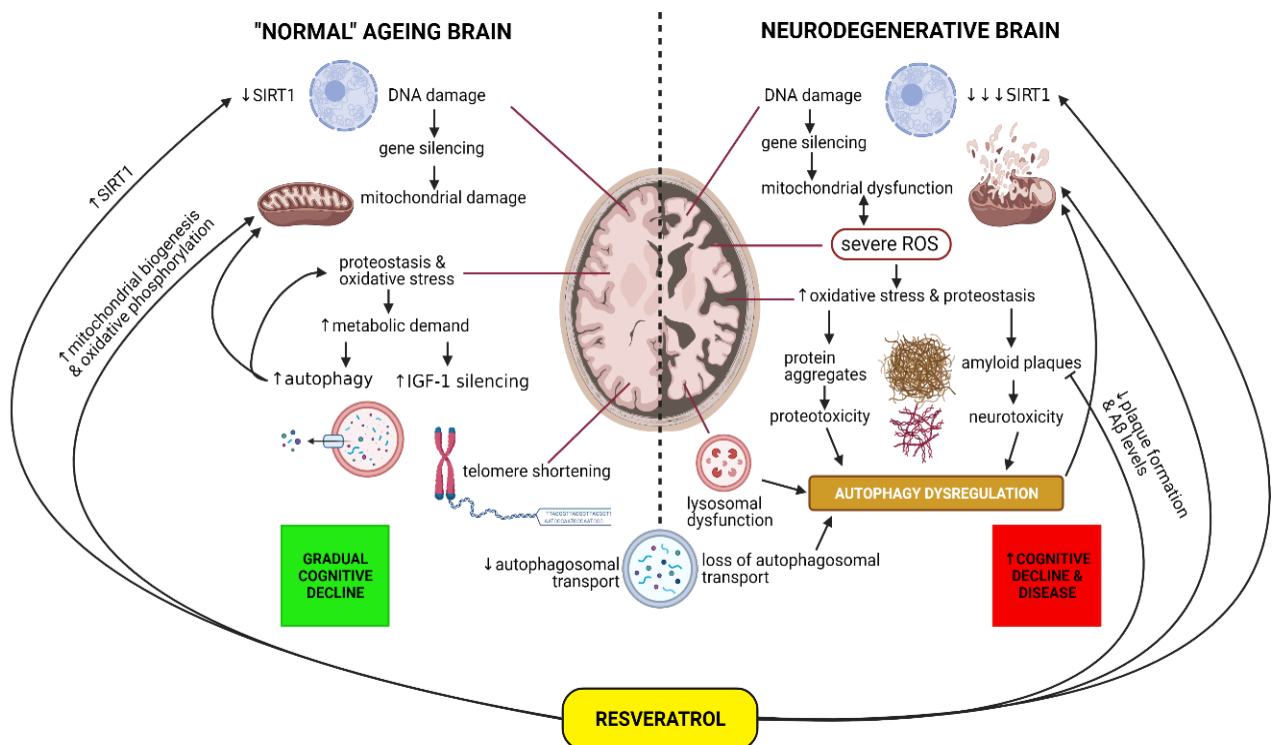
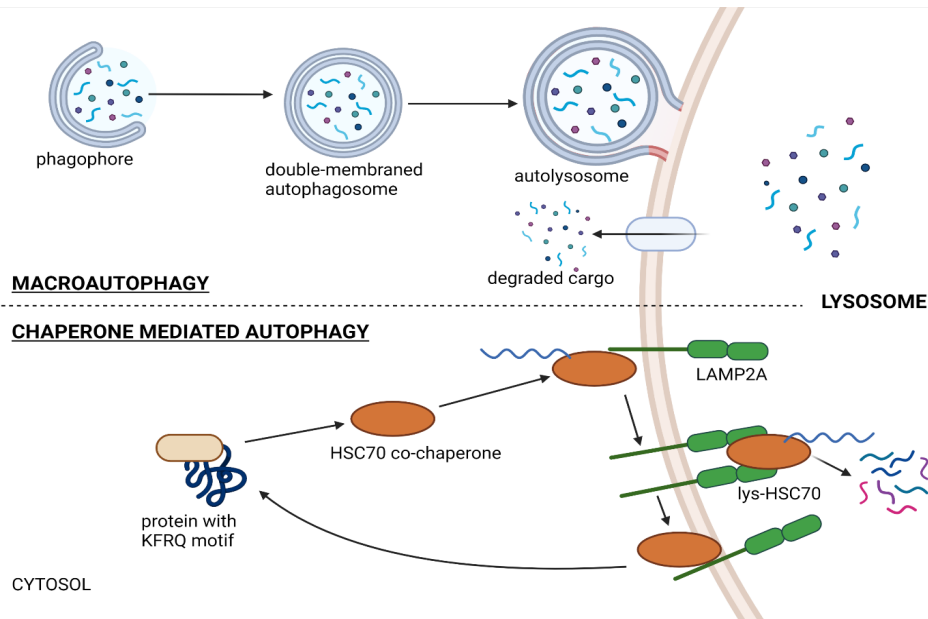


Figure 2.1: The hallmark features of ageing in comparison to ageing with neurodegeneration, which leads to an increase in cognitive decline and disease. The pathways with which the antioxidant resveratrol, interacts with the system is also demonstrated (Bishop et al., 2010) (created with BioRender.com).

Autophagy plays an integral role in the dysregulation that occurs within the cell during the development of neurodegenerative disease. Autophagy is derived from the Greek words ‘auto’ meaning oneself and ‘phagy’ meaning to eat. The process is defined as any cellular pathway where cytoplasmic material is delivered to a lysosome for degradation (Levine & Kroemer, 2008). The degradation of short-lived proteins makes use of the ubiquitin proteasome system (UPS), which degrades specific, tagged and ubiquitinated cargo (Kocaturk & Gozuacik., 2018). Autophagy holds many crucial homeostatic roles within the cell including acting as a buffer against starvation through the liberation of building blocks from macromolecules, the protection from cell death insults, permitting early embryonic development as well as it being a course of degradation for numerous infectious agents as well as aggregate-prone proteins (Rubinsztein et al., 2012). As of late three types of autophagy exist namely, chaperone mediated autophagy, microautophagy and macroautophagy.

Figure 2-2 below shows the sub-type macroautophagy, describes the major catabolic mechanism utilized by eukaryotic organisms to degrade long-lived proteins. The process begins with the formation and elongation of a phagophore, which following fusion forms the autophagosome, a double-membraned vesicle that sequesters cytoplasmic material. The autophagosome then fuses with a lysosome to form an autolysosome, where the cytoplasmic cargo along with the organelle’s inner membrane is degraded by acidic hydrolases (Levine & Kroemer, 2008).



**Figure 2.2: The autophagy process. Macroautophagy begins with the formation of a phagophore that following elongation, forms the autophagosome, a double-membraned vesicle capable of sequestering cargo. Upon fusion with a lysosome to form an autolysosome, the sequestered cargo is degraded by acidic hydrolases. The chaperone-mediated autophagy process begins with the specific targeting of proteins to a lysosome via signal peptides and coordinated chaperones (created with BioRender.com).**

Chaperone-mediated autophagy (CMA) requires specific targeting of various proteins to lysosomes via signal peptides and coordinated chaperones that are located on the targeted membrane. The pathway shown in figure () does not require membrane invaginations or vesicles as substrates are delivered to the lumen of the lysosome via a protein-translocation complex located on the membrane of the lysosome. The process is only capable of degrading soluble, KFERQ-like motif-containing proteins

which is present in ribonuclease A, and cannot degrade organelles. CMA functions in metabolic regulation, aging, T-cell activation and oncogenes and is able to degrade macromolecules including integral membrane proteins, lipids and, nucleic acids (Galluzzi et al., 2017).

Alzheimer's disease is the neurodegenerative disease characterized by senile plaques and neurofibrillary tangles (Nixon & Yang, 2011). Neurofibrillary tangles, that are found inside affected neurons, are composed mainly of an abnormally phosphorylated and aggregated form of the microtubule-associated protein tau. Senile plaques consist of deposited extracellular material distributed among the axons and dendrites in clusters (Nixon & Yang, 2011). The senile plaques also consist of the accumulation of dystrophic neurites which are filled with autophagic vacuoles (AV's). These vacuoles consist of various types of organelles including autophagosomes, multilamellar bodies and autolysosomes; all representing different stages of the autophagy process (Nixon & Yang, 2011).

With neurodegenerative disease, the autophagy process which is responsible for proteolytic clearance, is impaired. This leads to the accumulation of key proteins. In Alzheimer's disease it is the aggregation of Amyloid- $\beta$ . In Parkinson's disease, it is the accumulation of Lewy bodies which consist mainly of the protein  $\alpha$ -synuclein (Nixon & Yang, 2011). Huntington's disease also describes macroautophagy dysfunction, particularly alterations in the ability of the autophagosomes to recognize cytotoxic cargo (Martinez-Vicente et al., 2010). Low- and medium-income countries are especially affected by these diseases as many people cannot afford the costs such a chronic disease implies (Wortmann, 2012). This suggests a greater risk for South Africa, where this risk is further exacerbated by environmental factors such as water pollution.

## **2.2 INTERACTIONS BETWEEN HEAVY METALS, THE BLOOD BARRIER AND GASTROINTESTINAL TRACT**

The blood-brain barrier (BBB) is one of four mechanisms; along with the meninges, skull and cerebrospinal fluid; that is used to protect the brain from injury or trauma. The barrier separates the systemic blood circulation from the interstitial fluid (Zheng et al., 2003). It is also important to note the barrier that separates the systemic circulation from the cerebrospinal fluid compartment is known as the blood-CSF barrier (BCB). The BBB plays many integral roles in addition to the movement of materials such as the active participation in various brain functions and development, maintenance of the microneuronal environment, CNS homeostasis, fibrinolysis and coagulation and blood cell activation (Zheng et al., 2003). The regulation of blood-brain tissue exchange is accomplished by individual endothelial cells that are continuously linked by tight junctions known Zonulae Occludentes. For most solutes and macromolecules, permeability across the BBB is dependent upon their lipophilicity and size (Zheng et al., 2003). It is assumed that toxic metals enter the brain through the central nervous system (CNS).

Most metal species such as free metal ions and complexes of metal with an amino acid or protein, e.g. transferrin, are hydrophilic, meaning they cannot sufficiently be transported across the blood-brain barrier. Conversely, many metals are absorbed from the gastrointestinal tract (GIT) where they can enter the systemic circulation. The metal could then enter the CNS from the blood across the BBB or by crossing the choroid plexus into the cerebrospinal fluid, from which it can diffuse into the cerebrospinal fluid (Yokel, 2006). As protection, the body has developed various mechanisms to detoxify toxic substances, such as heavy metals, with various cells and the secretions of GIT playing an important role in the process. The cells of the body have also evolved a complex network of metal trafficking pathways, where the accumulation of metal in its freely reactive form is prevented and the

proper delivery of the ion to target metalloproteins through metal utilization pathways, is ensured (Upreti et al., 2004).

Many metals such as copper, manganese and iron are crucially required for the optimal functioning of the CNS. They play important roles such as catalysts, second messengers, gene expression regulators as well as being essential cofactors for functional expressions of many proteins. These metals are also needed to activate and stabilize enzymes, such as protein kinases, superoxide dismutase and metalloproteases (Yokel, 2006). It is therefore clear that both the excess and deficiency of these metals can result in the dysfunction of the CNS.

## 2.3 ROLE OF HEAVY METALS IN NEURODEGENERATION

### 2.3.1 Copper

Copper exists as a free, unbound metal ion and participates in the metabolism of neurotransmitters and nerve myelination (Zheng & Monnot, 2012). The biological mechanisms that regulate copper homeostasis take place in the processes of absorption, distribution, biotransformation and excretion. In the CNS, these processes are located primarily in the BBB (Zheng & Monnot, 2012). The body of a healthy adult possess approximately 110mg of copper, primarily distributed in the liver (10mg), brain (8.8mg), blood (6mg), bone (46mg) and muscle (26mg). Copper is also found in the cerebrospinal fluid (>70  $\mu\text{M}$ ) as well as in the brain extracellular space (1  $\mu\text{m}$ ) (Opazo et al., 2014). Various studies have shown that the concentration of serum copper is significantly higher in women ( $p < 0.05$ ) than in men (Angelova et al., 2011).

Copper ions are connected to proteins and ceruloplasmin by 95% and the remainder to albumin and amino acids (Angelova et al., 2011). The majority of copper ions are absorbed in the small intestine and delivered to the liver and kidneys (Zheng & Monnot, 2012). Dietary copper present in the form of  $\text{Cu}^{2+}$  is absorbed primarily into the body through the intestinal mucosal cells, and is delivered to the liver via the portal blood bound to albumin, transcuprein and, to lesser extent, amino acids and small peptides (Hung et al., 2010). Following copper absorption through the stomach and duodenum, it is rapidly removed from the portal circulation by hepatocytes in the liver (Madsen & Gitlin, 2007). The membrane-associated Copper transporters include copper transporter-1 (CTR1), DMT1 and Cu exporter ATPases (ATP7A and ATP7B). They are responsible for intestinal copper uptake. CTRL is a plasma membrane protein essential for early embryonic development and intestinal copper uptake and is present on the endothelial cells of the BBB (Madsen & Gitlin, 2007).

Intracellular copper metabolism is dependent on the copper transport ATPases, ATP7a and ATP7b. In the brain, ATP7a is expressed in endothelial cells of the BBB and facilitates copper movement across the basolateral membrane into the extravascular space of the brain. ATP7a is also expressed within specific populations of neurons in several brain regions including the cerebellum and hippocampus (Madsen & Gitlin, 2007). Intracellular trafficking of copper also requires proteins namely the metallochaperones which direct copper to specific cellular pathways. Chaperones include antioxidant protein-1, cytochrome oxidase enzyme complex and Cu chaperone for SOD. In the human body, copper exists in two forms – the first and second oxidation form, where most copper is in the second form (Angelova et al., 2011).

Copper is distributed throughout most regions of the brain and is most abundant in the basal ganglia (Madsen & Gitlin, 2007). In synaptic vesicles, copper can form complexes with neurotransmitters. For

example, copper can form ternary complexes with ATP and norepinephrine (Opazo et al., 2014). Once inside the cell, copper has four possible fates: It can enter the copper-metallothionein storage pool, it can be transported to the mitochondria for incorporation into cytochrome c oxidase, it can be incorporated into cytoplasmic Cu/Zn SOD, or it can be transported to a P-type ATPase in the trans-Golgi network for transport out of the cell (Zheng & Monnot, 2012).

Figure 2-3 demonstrates the various homeostatic roles of copper. Copper is a functional component of several essential enzymes, known as copper enzymes – cytochrome c oxidase, lysyl oxidase, feroxidase, 2-furoate-CoA dehydrogenase, amine oxidase, catechol oxidase, tyrosinase, dopamine beta-monooxygenase, D-galaktozo oxidase, D-hexozo oxidoreductase, indole 2,3-dioxygenase, L-ascorbatoxidase, nitratoreductase, peptidylglycine monooxygenase, flavonol 2,4-dioxygenase, superoxide dismutase, PHM (peptidylglycine monooxygenase hydroxylation) and other (Angelova et al., 2011). Superoxide dismutase (SOD) functions as an antioxidant, which catalyses the conversion of superoxide radicals (free radicals) in hydrogen peroxide, that can subsequently be reduced to water by other antioxidant enzymes. Two forms of SOD contain copper: 1) copper / zinc SOD is found in most cells of the organism, including red blood cells, and 2) extracellular SOD is a copper-containing enzyme, located in large quantities in the lungs and in low levels – in plasma (Angelova et al., 2011).

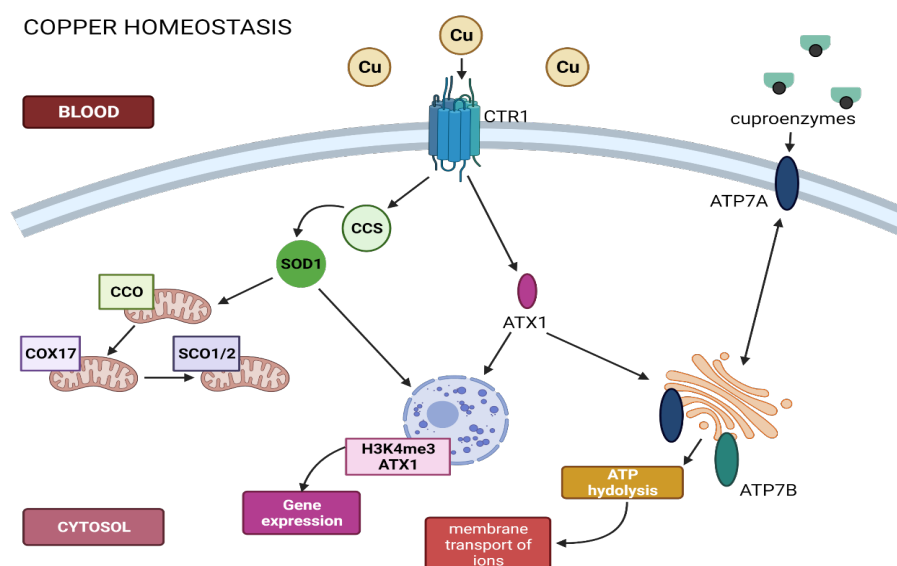


**Figure 2.3: The various homeostatic roles of copper inside the cell. With superoxide dismutase (SOD), copper is transported to the mitochondria and through the metallochaperone COX17, is used to ensure cytochrome c oxidase stability. The protein ATX1 transports copper ions to the nucleus for gene expression and to the Golgi body to assist in the transport of ions. Cuproenzymes also make use of copper components in regulating oxygen transport, redox reactions and cellular metabolism (Lutsenko, 2010)(created with BioRender.com).**

Delivery of copper to the mitochondria cytochrome oxidase, a key mitochondrial enzyme in the respiratory chain, requires a total of three copper ions to be inserted into two subunits: a binuclear copper site protruding into the inner membrane space of the mitochondria and a mononuclear site buried within the inner membrane (O Halloran & Culotta, 2000). The host of assembly factors required for cytochrome oxidase activity; two proteins clearly have an effect on copper utilization. One of these, COX17, is a candidate metallochaperone (O Halloran & Culotta, 2000). COX17 localizes to both the cytosol and inner membrane space of the mitochondria, consistent with a role as a shuttle protein for

delivering copper to mitochondria (O Halloran & Culotta., 2000). COX17 may act as the shuttle protein to deliver copper to mitochondrial factors such as SCO1/SCO2, which are responsible for the stability of cytochrome c oxidase.

ATX1 was found to specifically shuttle copper to an intracellular copper transporter located in the Golgi compartment of the secretory pathway. The targets of copper delivery by ATX1 are P-type copper transporters that are also conserved among eukaryotes. These transporters are members of a large family of transporting ATPases that use energy from ATP hydrolysis to drive membrane transport of ions. Humans express two forms of this transporter, known as ATP7A and ATP7B. Transport of ATX1 to the nucleus also enables gene expression through the epigenetic marker H3K4me3 (Lutsenko, 2010). The copper chaperone for SOD1 (CCS) is the largest of copper metallochaperones identified to date. CCS folds into three functionally distinct protein domains. Thus far, no eukaryotic chaperones for metals other than copper have been established (O Halloran & Culotta., 2000). Copper's ability to accept and donate single electrons make it an ideal redox cofactor, but copper ions are also complicit in the Fenton reaction and hence capable of driving the generation of deleterious hydroxyl radicals (Robinson & Winge, 2010).

Free copper is elevated in neurodegenerative disease Squitti and colleagues in Italy have done important work showing that mean non-ceruloplasmin plasma copper (called free copper) is elevated in Alzheimer's disease; free copper levels correlate with cognitive function in AD as measured by the Mini-Mental State Examination (MMSE)<sup>2</sup>; and free copper levels are predictive in decline of MMSE over time in patients with AD (Brewer et al., 2010). Figure 2-4 below demonstrates the dysregulation that occurs in the cell with excess copper in the cell, and its relation to neurodegenerative disease. Binding sites for copper were identified in amyloid plaques. Copper has a high affinity to amyloid- $\beta$  42.

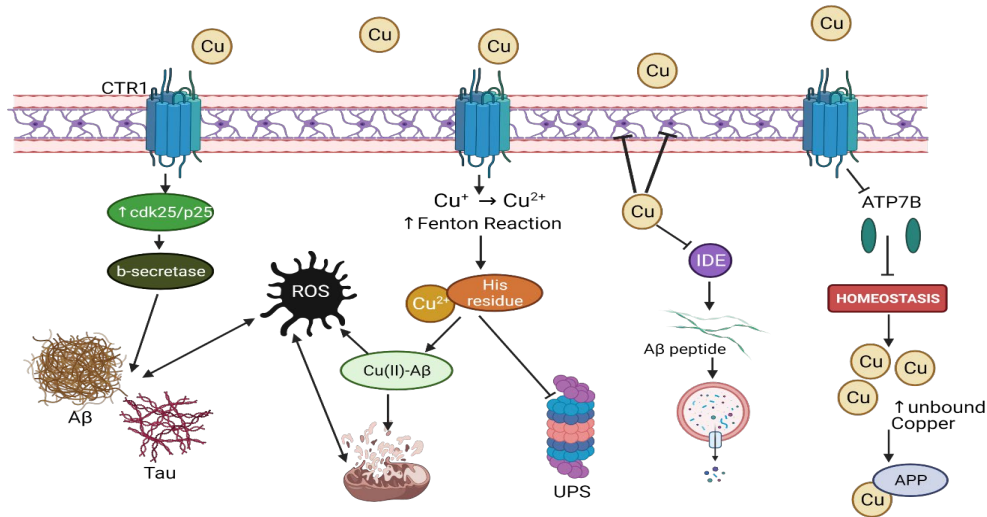


**Figure 2.4: The effects of excess copper on the cell. An increase in the Fenton reaction for copper with the additional dysregulation of the copper homeostasis, leads to an increase in unbound ions that are capable of binding to APP, Amyloid- $\beta$  and histone residues. The latter leads to a dysregulation in the functioning of the UPS system, as well as mitochondrial dysfunction and ROS generation. Excess copper is capable of increasing the activity of  $\beta$ -secretase, and inhibiting astrocyte functioning and insulin degrading enzyme (IDE) pathway responsible for cleaving A $\beta$ . This leads to a loss of the brains neuroprotective capabilities as well as an increase in protein aggregations, both of which are hallmark features for neurodegenerative disease (Brewer et al., 2010) (Pohanka, 2019)(Opazo et al., 2014)(Hsu et al., 2018)(created with BioRender.com).**

Copper is also capable of blocking A $\beta$  peptide degradation. Under normal conditions, zinc metalloprotease/insulin-degrading enzyme splits A $\beta$  42, but copper in the oxidative states I and II and silver ions act as inhibitors of the enzyme (Pohanka, 2019). In Parkinson's disease, the number of copper ions bound on one molecule of ceruloplasmin is reduced. Copper also induces  $\alpha$ -synuclein aggregation (Pohanka, 2019).

Only 20% of Alzheimer's disease cases are fully explained by currently known susceptible genes or mutations. Therefore, nonheritable, nongenetic factors are predicted to contribute considerably to triggering neurodegeneration and cognitive decline by interacting with susceptible genes and aging (Hsu et al., 2018). However, the identification of specific environmental risk factors for AD is extremely challenging because of the long latency of the prodromal and cognitively normal phase prior to the clinical manifestations of AD, and because exposure to environmental contaminants could be variable throughout life (Hsu et al., 2018). The preponderance of copper found in solid food is present in organic molecules as the cuprous Cu<sup>+</sup> form, while that found in drinking water is in the inorganic cupric Cu<sup>2+</sup> form. This difference in the valency of copper could result in differential mechanisms of absorption and distribution in the body (Hsu et al., 2018).

The brain also has additional network of proteins that bind to copper and control its homeostasis including amyloid precursor protein (APP) and prion protein. These proteins are considered as primary culprits for major neurodegenerative diseases, AD, and prion disease, respectively (Hsu et al., 2018). Less is known about the absorption of cupric (Cu<sup>2+</sup>), which is possibly absorbed through divalent metal transporter 1 or other shared metal transporters. Various copper chaperones distribute it to organelles and enzymes or excrete it from the cell via specialized copper transporters, ATP7A and ATP7B (Hsu et al., 2018). Recent genetic evidence to further support the link between copper dyshomeostasis and AD is the identification of polymorphisms in the ATP7B gene as an increasing risk for AD, and polymorphic ATP7B is suspected to functional alterations and perturbation of copper homeostasis (Hsu et al., 2018).

Discordance of copper levels in the cerebrospinal fluid, brain tissues, and serum in AD patients points to a systemic imbalance of copper homeostasis and impaired distribution of copper causing deficiency in the cerebrospinal fluid and excess free copper in the circulation which leads to the toxic mechanisms of action of copper, such as promoting A $\beta$  build-up and oxidative damage. The physical interaction and binding affinity of copper to extracellular domain of APP and A $\beta$  species have been extensively studied and shown to promote A $\beta$  production and fibrillization in vitro. Within the A $\beta$  sequence, the redox-active Cu<sup>2+</sup>, but not Cu<sup>+</sup>, is coordinated to the histidine (His6, His13, and His14) or Tyr10 residues. This coordination leads to formation of the Cu(II)-A $\beta$  complex (predominantly with 1:1 stoichiometry) and aggregation process that involves a conformational change. The colocalization of copper and Amyloid- $\beta$  in the glutamatergic synapse during NMDA-receptor-mediated neurotransmission provides a microenvironment favouring the abnormal interaction of redox-potent A $\beta$  with copper under conditions of copper dysregulation thought to prevail in the AD brain, resulting in the formation of neurotoxic soluble A $\beta$  oligomers. Interactions between A $\beta$  oligomers and copper can further promote the aggregation of A $\beta$ , which is the core component of extracellular amyloid plaques, a central pathological hallmark of AD.

Classically, the Cu(II)-A $\beta$  complex is thought to generate reactive oxygen species (ROS) and mediate oxidative damage through Fenton-type reaction and impairment of mitochondrial function. To date, although there is no evidence supporting a strong correlation between APP expression and brain copper levels in AD, Down syndrome, or individuals with APP duplication gene, recent studies carefully quantified copper in brain tissues by inductively coupled-plasma mass spectrometry and determined a significant reduction of copper in several brain regions including hippocampus, amygdala, entorhinal cortex, and cerebellum among AD patients (Hsu et al., 2018). In a 3xTg-AD mouse model, however, the high dose copper in drinking water induced detrimental effects including accelerated cognitive

impairment and increased A $\beta$  and tau build-up by upregulating the activities of a- and b-secretase and by activating cdk5/p25. Thus, removing excess copper could be a potential therapeutic intervention to ameliorate AD neuropathology. Preclinical testing of metal chelators, clioquinol and DP-109, demonstrated a significant reduction of cerebral A $\beta$  deposit in Tg2576 mice. Chronic exposure to 0.13 ppm copper in drinking water in APP23 transgenic mouse model revealed elevated levels of non-Cp-bound Cu in plasma and subsequent downregulation of low-density lipoprotein receptor-related protein 1 (LRP1) in capillary endothelial cells. A parallel loss of LRP1 is observed in advanced aging and in AD brains.

A study using murine monocyte BV2 cells reported that Cu<sup>+</sup> can polarize cells from a proinflammatory M1 phenotype to a protective anti-inflammatory M2 phenotype via inhibition of nitric oxide production. Conversely, BV2 cells exposed to Cu<sup>2+</sup> had impaired phagocytosis and increased release of proinflammatory cytokine, such as IL-1b, IL-6, and TNF $\alpha$ , following A $\beta$  stimulation. Astrocytes can actively restore and resist against Cu-induced toxicity in part because astrocytes have a high capacity to uptake excess copper via CTR1 and sequestering it in glutathione and metallothionein complex, key endogenous antioxidant molecules to protect cells against ROS. Astrocyte dysfunction by ageing or other means, together with environmental Cu exposure may result in the loss of neuroprotective and antioxidative capacity of the brain and increased susceptibility to cognitive decline and AD (Hsu et al., 2018). Ubiquitin plays a critical role in protein degradation driven by 26S Proteasome. UPS dysfunction is associated with neurodegenerative disorders. The study by Kojima et al., strongly suggested that Cu<sup>2+</sup>, as a part of one metal complex, is coordinated by ubiquitin with the participation of a histidine residue further suggesting that copper might participate upstream in the regulation of UPS (Opazo et al., 2014).

Studies have that the concentration of total copper is decreased in the brain of AD patients, while the concentration of labile copper is increased in the most affected regions of the AD brain. Cu<sup>2+</sup> ions bind to  $\beta$ -amyloid peptides with high affinity and increase the proportions of  $\beta$ -sheet and  $\alpha$ -helix structures in amyloid peptides, which can be responsible for  $\beta$ -amyloid aggregation. Various concentrations of Cu<sup>2+</sup> ions enhance fibril formation while binding of copper ions to  $\beta$ -amyloid noticeably increases its toxicity for cells. Fibril formation is highly pH-dependent and Cu<sup>2+</sup> ions cause it to occur at physiological pH. However, the formation of amorphous aggregates dominates in acidic conditions. Fibril formation is highly pH-dependent and Cu<sup>2+</sup> ions cause it to occur at physiological pH. However, the formation of amorphous aggregates dominates in acidic conditions (Bagheri et al., 2018).

The production of Reactive Oxygen Species (ROS) is a key factor in  $\beta$ -amyloid toxicity toward neurons, which is dependent on metal ion redox properties. Copper ions in complex with  $\beta$ -amyloid fibrils produce hydrogen peroxide, in the presence of biological reducing agents. When the ratio of copper to peptide increases, hydrogen peroxide levels and the production of hydroxyl radicals increase, and the morphology of aggregates changes from fibrillar to amorphous (Bagheri et al., 2018). HNE, which is a product of x-6 PUFA oxidation, promotes both membrane association and A $\beta$  fibril formation. HNE is produced by A $\beta$ -copper complexes in contact with lipid membranes, HNE modifications on A $\beta$  occurs mainly at the His residues. An excess in copper is also found to inhibit the metallochaperone insulin-degrading enzyme (IDE), which when forming a subunit with zinc, is responsible for the cleaving of A $\beta$  peptides (Grasso et al., 2017).

Copper is a redox-active metal that participates in diverse metabolic processes in living organisms. Some of the key cuproenzymes include cytochrome c oxidase (CCO; electron transport and oxidative phosphorylation), Cu and Zn superoxide dismutase (Cu, Zn-SOD; antioxidant defence), tyrosinase (pigmentation), ceruloplasmin (iron transport and radical scavenging) and dopamine b-hydroxylase (neurotransmission). Paradoxically, the redox property of copper means copper can also catalyse the

production of ROS such as hydroxyl radicals via participation in Fenton or Harber-Weiss reactions (Hung et al., 2010). Copper-tau interaction has been hypothesised to induce the development of intracellular NFTs, the other characteristic hallmark of AD (Hung et al., 2010).

### 2.3.2 Cadmium

In the 1960s cadmium was catapulted into the mainstream of metal toxicology research when it was identified as the major etiological factor in itai itai disease, a condition that afflicted Japanese women exposed to cadmium via their diet which contained cadmium contaminated rice and water (Rani et al., 2014). Chemically similar to zinc and mercury, cadmium is an important component in the production of Ni-Cd rechargeable batteries and corrosion-protection coating for iron and steel. It is found in most soil and rocks, coal, mineral fertilizers and cigarette smoke. During recent decades, anthropogenic activities such as agriculture and mining have significantly increased its dispersal in soil and water. Cadmium is not a physiological element for any living organism and due its slow excretion from the human body, a long biological half-life of 10-30 years and high solubility in water, is defined as a cumulative toxicant, capable of heavily aggregating in various organs (Rani et al., 2014)(Forcella et al., 2020)(Polykretis et al., 2019). The metal has also been listed as the seventh most hazardous chemical for human health (Forcella et al., 2020).

One of the first evidences for a relationship between cadmium uptake and neurodegeneration was reported in 2001 in a patient with Amyotrophic Lateral Sclerosis-like syndrome after occupational cadmium intoxication (Forcella et al., 2020). Severe exposure to cadmium can result in may result in pulmonary effects such as emphysema, bronchiolitis and alveolitis. Renal effects are also associated with cadmium exposure from inhalation and ingestion (Singh et al., 2010). In the Kempen region between Belgium and the Netherlands, there was an increased cadmium content of locally grown vegetables from air pollution, surface water pollution and solid waste build up and exposed individuals were found to have kidney malfunction (Genthe et al., 2018). The gathered knowledge on cadmium neurotoxicity has however not yet clarified the overall vision of the key events and processes necessary to untangle causes and consequences in a complex disease progression such as neurodegeneration (Forcella et al., 2020).

Dermal absorption of cadmium is generally very low at 0.1-0.8%, with the absorption of approximately 3-5% of cadmium from food and drink in the digestive tract. Once absorbed, cadmium is rapidly cleared from the blood and concentrates in various tissues, especially the liver and kidneys. While most cadmium is excreted via the bile system, following exposure and uptake into the systemic circulation, the cadmium that is left behind is initially bound to albumin in blood plasma followed by its uptake in blood cells (Rani et al., 2014). Figure 2-5 demonstrates the various effects of cadmium of the brain and brain cells. Cadmium can hardly enter the brain due to the protection of the BBB. However, it was reported that BBB-permeability is enhanced by chronic exposure to cadmium (Minami et al., 2000). Cadmium ions can enter into cells through the voltage-dependent  $Ca^{2+}$  channels which up-regulates IP3R1 (inositol 1,4,5-trisphosphate receptor) expression, which is capable of inducing  $Ca^{2+}$  release from endoplasmic reticulum (ER).

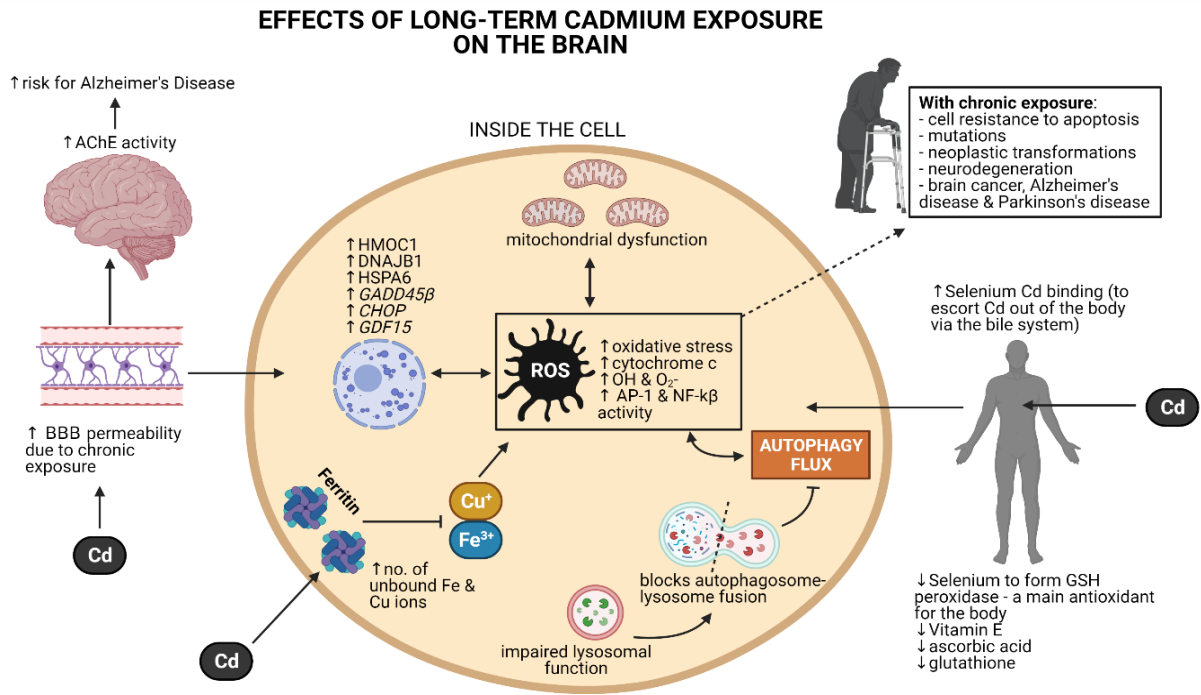


**Figure 2.5: The various effects of cadmium on the brain and the cells of the brain. An excess of cadmium increases BBB permeability which over time leads to excess cadmium in the brain. This has shown to increase Acetylcholinesterase activity which is a known risk for Alzheimer's disease. Inside the cell, cadmium affects the nucleus by upregulating various genes which code for proteins that are responsible for inflammation and oxidative stress (HMOC1), proteotoxic stress (DNAJB1 and HSPA6), DNA damage (GADD45 $\beta$ ) and markers of neurodegeneration (CHOP and GDF15). Cadmium has also shown to impair lysosomal function which results in autophagosome-lysosomal fusion and blocks autophagy flux. The end-result leads to an increase in ROS and oxidative stress, a decrease in various integral antioxidants. With chronic exposure in the brain through these mechanisms, there is an increased risk for brain cancer and neurodegenerative disease (Carageorgiou et al., 2005)(Forcella et al., 2020)(Polykretis et al., 2019)(Rani et al., 2014)(created with BioRender.com).**

Cadmium is known to affect the cell proliferation and differentiation, cell cycle progression, DNA synthesis, apoptosis and the inhibition of DNA repair (Rani et al., 2014). In a study by Forcella et al., it was shown that cadmium induces a strong deregulation of specific transcripts, mostly being metallothioneins which are involved metalloregulatory processes. Heme-oxygenase 1 (HMOX1) was amongst the top upregulated genes. This is of research interest due to the fact that this gene encodes for the protein heme-oxygenase-1 (HO-1), which is considered a major protein in diseases caused by oxidative stress and inflammation. Another group of upregulated stress-related genes is represented by ZFAND2A, HSPA1A, HSPA6, HSPA1B, DNAJB1 which belongs to a superfamily of cytoprotective chaperones that code for heat shock-related proteins, dealing with proteotoxic stress.

The product of growth arrest and DNA damage response 45 $\beta$  (GADD54 $\beta$ ) gene involved in regulating autophagy and apoptosis in rat cerebral neurons and cell growth arrest and DNA repair, was among the highest upregulated genes (Forcella et al., 2020). Lastly, other genes found among the top upregulated in cells exposed to cadmium include CHOP and GDF15, both of which are linked to neurodegeneration. CHOP has been linked to the activation of apoptosis signalling in neuroblastoma

cells and GDF15 levels in the cerebrospinal fluid has been proposed as a potential marker in disorders such as Parkinson's disease.

Among the down-regulated genes, a group of cadmium-targeted genes encodes for neuronal-related proteins: GREM2 codes for the gremlin protein family, described as neuroprotective factors in dopaminergic neurons both in vivo and in vitro (Forcella et al., 2020). SH-SH5Y neuronal cells exposed to cadmium induces stress by activating the heat shock proteins and metallothioneins, both acting as the first line of defence against cadmium and metals in general. The high response of various heat shock proteins such as increased Hsp70 following cadmium exposure, suggests the need of these molecular chaperones to refold mis-folded proteins and degrade damaged or aggregated proteins. The perturbation of protein homeostasis and protein folding, aggregation and degradation may lead to accelerated ageing and proteotoxicity-triggered disorders, both of which are hallmarks of neurodegenerative disease (Forcella et al., 2020).

While cadmium is unable to generate free radicals by itself, it is capable of indirectly generating the superoxide radical, hydroxyl radical and nitric oxide radicals (Rani et al., 2014). Unlike copper, cadmium is not a Fenton-like metal and it is therefore not directly involved in the production of ROS. Cadmium is in fact thought to be responsible for the replacement of metals from their catalytic sites, the depletion of antioxidant metabolites such as glutathione, ascorbic acid and vitamin E, the inhibition of the electron transport chain which results in mitochondrial damage and, the alteration of the enzymatic activity of antioxidant proteins (Polykretis et al., 2019).

In vitro, cadmium has been shown to bind to the zinc and copper sites of SOD1, which are necessary for the structural stability and catalytic activity and SOD1 (Polykretis et al., 2019). At the cellular level, cadmium induces both the damaging and repair processes in which the cellular redox status plays an important role (Rani et al., 2014). Redox-inactive metals such as lead, cadmium, mercury and others deplete cell's major antioxidants, particularly thiol-containing antioxidants and enzymes. Either redox-active or redox-inactive metals may cause an increase in production of reactive oxygen species (ROS) such as hydroxyl radical ( $\text{HO}^\cdot$ ), superoxide radical ( $\text{O}_2^\cdot^-$ ) and hydrogen peroxide ( $\text{H}_2\text{O}_2$ ). Enhanced generation of ROS can overwhelm cells' intrinsic antioxidant defences, and result in a condition known as oxidative stress in cells that can be partially responsible for the toxic effects of heavy metals (Rani et al., 2014).

Another study reported that the treatment of HL-60 cells with cadmium resulted in the appearance of cytochrome c (Rani et al., 2014). Cadmium is also capable of replacing the iron and copper from a number of cytoplasmic and membrane proteins like ferritin, which in turn would release and increase the concentration of unbound iron or copper ions. These free ions participate in causing oxidative stress via the Fenton reactions (Rani et al., 2014). Cadmium stimulates calcium-permeable AMPA/kainite receptors, which means it might also trigger GABA release even under inhibition of the voltage-dependent calcium channels with cadmium (Minami et al., 2000). L-Cysteine (Cys) is an antioxidant agent believed to form a relatively stable chelator-metal complex with metals such as cadmium, thereby assisting in the excretion of the latter and resulting in a decrease of cadmium in the tissue (Carageorgiou et al., 2005).

Acetylcholinesterase is a crucial enzyme for cholinergic neurotransmission, it is also co-released with dopamine from the dopaminergic neurons, thus emphasizing the interaction between the two. AChE is also involved in cell survival, neurite growth and voltage-dependent calcium currents (Carageorgiou et al., 2005). Areas of higher AChE expression generally correlates with brain regions that degenerate early in Alzheimer's disease (Carageorgiou et al., 2005). It was shown by Carageorgiou et al., that long-

term cadmium administration increased AChE activity in the rat brain, and lowers the brains total antioxidant status (however when administered with zinc and calcium, the status stays the same).

The UPS is a highly conserved cellular pathway that plays an important role in the selective degradation of cellular proteins that are essential for the regulation of a variety of vital cellular functions. Cadmium has shown that the perturbation of the UPS is important in mediating metal-induced cytotoxicity and apoptosis. The progressive accumulation of ubiquitinated protein conjugates has been associated with pathologic observations within humans, including brain aging and neurodegenerative diseases (Yu et al., 2009). Cadmium has shown to inhibit autophagy flux in neuro-2a cells. In the study by Pi et al., it was shown that cadmium administration increased the proteins p62 and LC3-II, both of which are autophagy markers.

To further detect autophagic flux, the study measured the level of LC3-II or GFP-LC3 puncta in the absence or presence of Chloroquine and it was found that 50  $\mu$ M Cd-induced accumulation of LC3-II or GFP-LC3 puncta was not significantly enhanced in the presence of Chloroquine. Cadmium decreases the co-localisation of LAMP-1, a lysosomal marker, with GFP-LC3 and has shown to significantly decrease LAMP-1, suggesting that cadmium is capable of reducing lysosome size. Using a LysoSensor Green, the study found that cadmium also increases the pH of lysosomes, indicating a reduction in lysosomal capability to perform its degradative functions (Pi et al., 2017).

Lastly, excess cadmium could result in the depletion of the mineral selenium in the body. Selenium atoms combine with cadmium atoms and are escorted out of the body via the bile system. Therefore, there is less selenium to form GSH peroxidase, one of the body's main antioxidants. This results in the formation of greater levels of ROS and hydrogen peroxide (Rani et al., 2014). The resulting oxidative stress leads to the activation of transcription factors such as AP-1 and NF-kB. It has been shown that cadmium-transformed cells are characterized by increased resistance to apoptosis, which may render them more prone to accumulation of mutations and neoplastic transformations that ultimately leads to cancer and neurodegenerative diseases such as Alzheimer's disease and Parkinson's disease (Rani et al., 2014).

The study of Genthe et al. (2018) analysed the heavy metal constituents in the water taken from the Limpopo Province. Cadmium was amongst the highest metal concentrations found and the mean concentration of cadmium in water sources in South Africa, namely villages near Hoedspruit in the Limpopo province, exceeded the guidelines for safe levels of intake as recommended by the World Health Organization (Genthe et al., 2018). This suggests that the cadmium levels in the drinking water of this region, as well as the water used for agriculture is in excess and may result in various negative outcomes for human health. The precise mechanism by which copper and cadmium alters behaviour and causes CNS disorders remains to be elucidated. There is also no effective therapy for cadmium poisoning.

### **2.3.3 Manganese**

Manganese is a heavy metal used in the manufacturing of steel, glass, batteries and ceramics (Chen et al., 2015). It is found in all body tissues and is essential in the synthesis of proteins, amino acids, lipids and carbohydrates (Dobson et al., 2004). Manganese is required for several physiological processes including brain and skeletal development, blood clotting, neuronal functioning and anti-viral innate immunity (Martins et al., 2019). Manganese intake for humans is primarily through dietary sources. Foods such as rice, nuts, legumes and whole grains contain the highest amounts of Mn (Chen et al., 2015). These dietary sources maintain an adequate level of manganese in humans, a 2.3mg/day requirement for men and 1.8mg/day for women (Aschner and Aschner, 2005). The estimated

distribution of manganese in the body is approximately 4-12ug/L in the blood, 1-8ug/L in urine and 0,4-0,85ug/L in serum (Martins et al., 2019).

Blood manganese is predominantly bound to  $\beta$ -globulin and albumin (Dobson et al., 2004). Manganese is mostly found in tissues rich in mitochondria and pigmentation such as bone, the kidneys, pancreas and liver, where most manganese is excreted in bile (Dobson et al., 2004). In the brain, manganese is predominantly deposited in the astrocytes via the high affinity transporter system (Zhang et al., 2020). Most excess manganese accumulates in the basal ganglia, with accumulations also being found in the globus pallidus, hippocampus and substantia nigra (Dobson et al., 2004). Airborne manganese can exist as fumes, aerosols or suspended in particulate matter. Manganese “dust” can be inhaled and deposited in the respiratory tracts, where the manganese can then be absorbed into the bloodstream (Dobson et al., 2004).

Manganese has three known sites of entry into the brain. The cerebral capillaries, the CSF via the choroid plexus and the olfactory nerve. Acute bolus intravenous injections of excessive manganese lead to a saturable transferrin-independent transport across the blood-brain barrier through active or passive processes (Dobson et al., 2004). Manganese plays a significant role in the changes in the level of activity of several antioxidant enzymes, such as superoxide dismutase, glutamine synthase, arginase and pyruvate carboxylate (Chen et al., 2015)( Martins et al., 2019). These metalloproteins are important for enzymatic processes that regulate development, immune function, antioxidant defences and energy metabolism (Chen et al., 2015). There are various transport mechanisms to buffer manganese levels to ensure homeostasis. Approximately only 1-5% of the manganese ingested by humans is absorbed into the body by the gastrointestinal tract.

Various factors affect manganese absorption, such dietary manganese levels, dietary levels of various minerals, age and iron status (Dobson et al., 2004). Several studies have demonstrated that iron deficiency increases manganese transport into the body as well as delivery to the brain (Dobson et al., 2004). Manganese enters the cell through several transports namely divalent metal transporter 1 (DMT1), transferrin receptor (TfR), the zinc transporters ZIP8 and ZIP14, the dopamine transporter (DAT), calcium channels, citrate transporters and the choline transporter. Among these, DMT1 is the primary transporter for divalent manganese and TfR is the primary transport for trivalent manganese (Chen et al., 2015). DMT1 is responsible for the mediation of the transport of various substrates such as manganese, copper, cadmium, iron, cobalt, zinc, lead and nickel (Chen et al., 2015).

The transporter is mainly expressed in the basal ganglia of the brain and has shown increased levels with age (Chen et al., 2015). It is also important to note that DMT1 has a higher transport affinity for manganese than it does for iron (Chen et al., 2015). Transferrin/transferrin receptor system transports trivalent manganese, which accounts for about 20% of total manganese in the blood. TfR is expressed in most cells, including neurons, astrocytes, microglia and the endothelial cells of the BBB (Chen et al., 2015). Endosomal  $Mn^{3+}$  is reduced to  $Mn^{2+}$  by ferrireductase, most likely to avoid the transport of trivalent manganese to the cytosol, which is a cause of oxidative stress. Divalent manganese is transported to the cytosol by endosomal DMT1 (Chen et al., 2015).

With regards to manganese export, this efflux it a crucial process to ensure the regulation of cellular levels of essential metals. This is emphasized through the genetic defects in efflux transporters as it typically results in hereditary disorders of metal metabolism such as Wilson’s disease and Menke’s disease (Chen et al., 2015). Four transporters have indicated manganese efflux activity in several experimental systems namely, ATPase 13A2, ferroportin, SLC30A10 and the secretory pathway calcium ATPase 1. ATPase13A2 is responsible for transporting manganese from the cytosol to the lumen of lysosomes (Chen et al., 2015). To date, the loss of function mutations in SLC30A10 are the

only known cause of a hereditary manganese-induced parkinsonian syndrome (Chen et al., 2015). The expression of SLC30A10 wildtype has shown to protect dopaminergic neurons against manganese-induced neurodegeneration (Chen et al., 2015).

The earliest symptoms of manganese toxicity are psychiatric. These include compulsive or violent behaviour, hallucinations and emotional instability. In addition, patients suffer from fatigue, muscle cramps, headaches, apathy and insomnia (Dobson et al., 2004). Severe manganese toxicity presents with dystonia, mild tremors and a signature 'cock-like' walk (Guilarte, 2010). A distinguishing feature of manganism is the lack of efficacy that levodopa, a drug used to treat PD, has in treating patients. Current treatment options are utilising a combination of levodopa and chelation therapy with edetate calcium disodium (EDTA) or para-aminosalicylic acid (PAS) (Chen et al., 2015). Manganese deficiency has also been associated with increased seizures, and skeletal defects (Martins et al., 2019). Manganese contributes to oxidative stress by increasing the production of nitric oxide through the activation of the inducible nitric oxide synthase in astrocytes (Martins et al., 2019).

Earlier studies have also indicated that following manganese exposure, the NF- $\kappa$ B pathway in astrocytes stimulate the production of inflammatory cytokines and chemokines such as IL-6, TNF, CCL2 and CCL5. Manganese exposure is also capable of increasing mRNA expression of pro-inflammatory cytokines IL-1 $\beta$ , COX-2 and TNF- $\alpha$  (Martins et al., 2019).

Excessive manganese exposure can directly cause free radical formation as a result of the redox-active nature of manganese as a transitional metal. Balmus et al., recently indicated that high manganese levels in Alzheimer's disease patients were strongly correlated with low antioxidant defences, demonstrated through decreased glutathione peroxidase activity. Manganese-induced oxidative stress can also result in mitochondrial dysfunction in neurodegenerative diseases. Mn<sup>2+</sup> interferes with calcium homeostasis within the mitochondria, which increases the mitochondrial calcium levels, interfering with oxidative respiration and inducing further oxidative stress. The excessive ROS generated by increased levels of manganese promote the opening of the mitochondrial permeability transition pore, resulting in a loss of membrane potential, a dysregulation of ATP synthesis, mitochondrial swelling and cellular apoptosis (Zhang et al., 2020). Mitochondrial homeostasis is further perturbed by the inhibition of the electron transport chain (Martins et al., 2019). Furthermore, this suggests that manganese may trigger apoptotic neuronal cell death as a result of mitochondrial dysfunction (Dobson et al., 2004).

Studies have also shown increases in plasma A $\beta$  peptides associated with an increased concentration of manganese (Martins et al., 2019). Conversely, there are also studies that suggest that manganese exposure leads to a decreased viability and lower expression of APP, which could limit non-amyloidic cleavage (Martins et al., 2019). Additional studies are needed to further elucidate the effects of the interactions of manganese and A $\beta$  on A $\beta$  aggregation and the associated molecular mechanisms.  $\alpha$ -Synuclein is a chaperone protein that is widely expressed in neural tissue where primarily localizes to the presynaptic terminal. It plays several crucial roles in dopaminergic neurotransmission, vesicle transport and the regulation of synaptic plasticity (Martins et al., 2019).

The aggregation of  $\alpha$ -synuclein is a hallmark feature in the pathology of PD. Mn<sup>2+</sup> has shown to trigger the misfolding and aggregation of  $\alpha$ -synuclein. Manganese exposure also promotes synuclein secretion in exosomal vesicles, which results in inflammation and neurodegenerative disease (Martins et al., 2019). The cholinergic system plays an integral role in cognitive domains associated with memory, learning and attention (Martins et al., 2019). Manganese perturbs the cholinergic system, resulting in locomotor, cognitive, behavioural and emotional dysfunction through modifying the enzymes involved in cholinergic transmission such as AChE (Martins et al., 2019).

Excessive manganese exposure causes a variety of effects in the striatum, but also causes abnormalities in GABAergic transmission in the globus pallidus, where manganese is found to accumulate the most in the basal ganglia (Martins et al., 2019). The neurotransmitter system that has been investigated the most with regards to manganese neurotoxicity is the dopaminergic system (Martins et al., 2019). DMT1 upregulation has been postulated to be involved with oxidative stress and dopaminergic cell loss, indicating that the transporter may contribute to neurodegeneration (Martins et al., 2019). The study by Zhang et al., who used mouse primary astrocytes, found that manganese suppressed manganese TFEB activity, which in turn resulted in the inhibition of autophagy flux. Manganese administration resulted in a significant reduction in LC3-II flux and LC3-1 expression and an increase in SQSTM1, a cargo receptor protein responsible for the degraded ubiquitinated proteins (Zhang et al., 2020). Manganese exposure down-regulates autophagy in primary astrocytes and impairs lysosomal function by reducing lysosome abundance and inhibiting proteolytic capacity (Zhang et al., 2020). Manganese exposure also inhibits nuclear localisation and transcriptional activity of TFEB, thereby reducing nuclear TFEB protein levels. This was seen through the manganese-induced elevated levels of phosphorylation of MAPK1/3, the main protein kinase responsible for the phosphorylation of TFEB, which results in the blockage of TFEB nuclear translocation. This dysregulation is believed to underly manganese-induced autophagic failure and mitochondrial dysfunction (Zhang et al., 2020) (Figure 2-6).

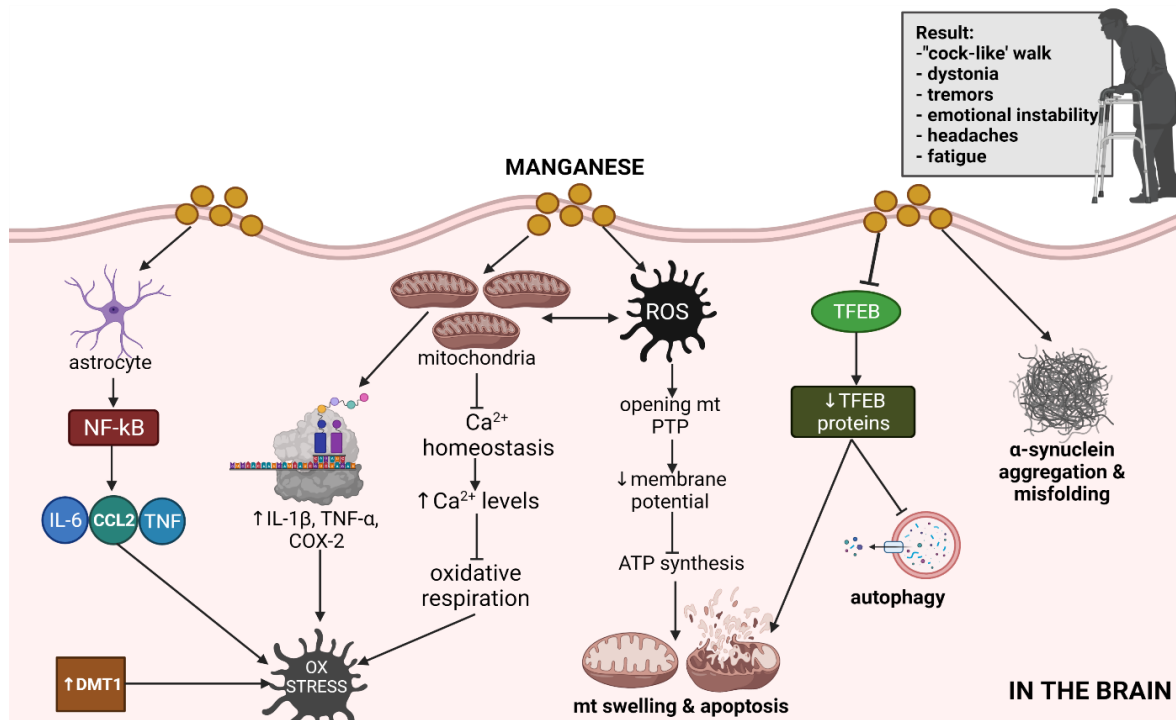


**Figure 2.6: The dysregulation of excess manganese in the brain. Manganese triggers the release of pro-inflammatory cytokines as well as their mRNA translation resulting in excess inflammation and oxidative stress which ultimately leads to mitochondrial dysfunction and apoptosis. With the increase in circulating manganese is the increase in metal transporters. Autophagy regulators such as TFEB are inhibited leading to the accumulation of neurodegenerative proteins (Dobson et al., 2004)(Zhang et al., 2020)( Martins et al., 2019)(created with BioRender.com).**

#### 2.3.4 Arsenic

Arsenic is ranked first among toxicants posing a significant potential threat to human health based on known or suspected toxicity (Tyler & Allan, 2014). Arsenic occurs within over 200 naturally occurring minerals, including the common occurrence of arsenic-bearing sulphide minerals within the gold deposits (Lanyon, 1997). Dissolved arsenic levels in aquatic ecosystems in many developing countries have been reported to be higher than the permissible limit (10 µg/L) set by World Health Organization (WHO) (Thakur et al., 2021). Low to moderate levels of arsenic exposure (10-300 µg/L) through drinking water has adverse effects such as skin lesions, circulatory disorders, neurological complications, diabetes, respiratory complications, hepatic and renal dysfunction including mortality due to chronic diseases. An estimation of about 100 million population all around the world are exposed to arsenic levels more than 50 µg/L via drinking water (Abdul et al., 2015).

Low doses and long-term exposures of arsenic leads to a range of medical complications termed as “arsenicosis” (Abdul et al., 2015). Specifically in South-east Asian countries, such as China, India, Bangladesh, Thailand and Taiwan, about 200 million people are at risk of arsenic exposure due to consumption of water containing arsenic more than permissible limits (Prakash et al., 2016). The first symptoms of exposure to arsenic in drinking water include pigmentation changes and hyperkeratosis, which reportedly appear after 5-10 years of exposure (Vahter, 2008). Inorganic arsenic is a well-documented potent human carcinogen, causing cancer in skin, lungs, urinary bladder, kidney and, possibly, liver (Vahter, 2008). Arsenic is absorbed mainly in the small intestine with minimal absorption through skin contact and inhalation (Prakash et al., 2016).

Ingestion, inhalation and skin absorption are some of the crucial routes for arsenic entering human body. Both pentavalent and trivalent arsenic compounds are rapidly and extensively absorbed from the gastrointestinal tract (Abdul et al., 2015). Binding of arsenic with certain metals and charged ions such as Ca or Mg promotes the adsorption of As(V) in the solid particulate phases (Thakur et al., 2021). Inorganic arsenic is reduced from arsenate to arsenite with the enzyme arsenate reductase mediated by glutathione (GSH), which further undergoes oxidative methylation through the enzyme arsenite methyltransferase mediated by S-adenosyl methionine, with conversion to MMA and DMA. Finally, all the metabolites are excreted through urine, among which DMA is the major metabolite (60-80%).

The toxic potential of arsenic primarily depends on the form of arsenic in the body. Arsenic initially absorbed through various routes enters the blood stream and is taken up by red blood cells (RBC), white blood cells (WBC), and other cells (Thakur et al., 2021). About 70% Arsenic (both organic and inorganic types) excreted through renal system via urine. Inorganic arsenic retains in the body longer than organic arsenic and excretion process of inorganic arsenic is longer (Abdul et al., 2015). Moreover, ingestion of inorganic arsenic may lead to tumorigenesis in various body parts such as skin, bladder, kidneys, lungs and liver along with other circulatory and neurological complications (Abdul et al., 2015).

The brain is a key target organ of arsenic toxicity affecting learning and concentration due to its ability of crossing blood brain barrier easily, with the highest accumulation being observed in the hypophysis (Abdul et al., 2015). Several animal studies have shown that arsenic exposure leads its accumulation in the brain (Prakash et al., 2016). Increased arsenic levels in the cortex, hypothalamus, striatum, cerebellum and hippocampus regions have been seen in rat brain after the administration of 100 ppm sodium arsenite for 60 days (Prakash et al., 2016). Figure 2-7 demonstrates the effects of excess or chronic exposure to arsenic.

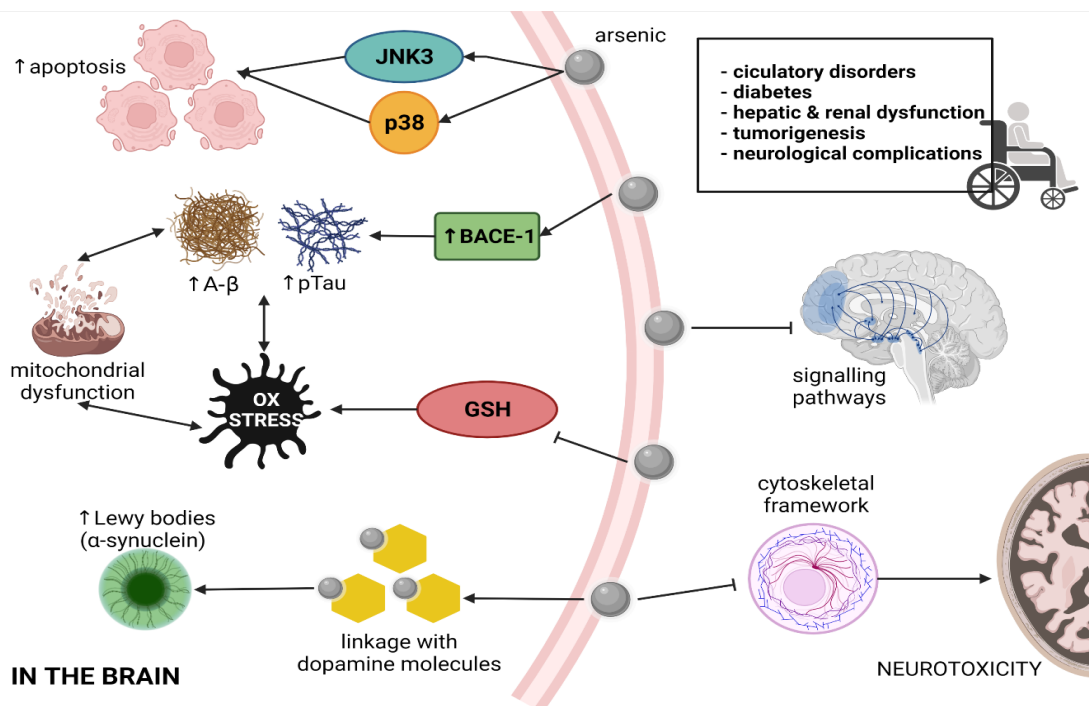


**Figure 2.7: The neurotoxicity caused by excess arsenic or chronic exposure to arsenic in the brain. Arsenic inhibits the functionality of anti-oxidants and upregulates apoptotic proteins and BACE-1, resulting in an accumulation of neurodegenerative proteins, an increase in oxidative stress and mitochondrial dysfunction. It also inhibits various brain signalling pathways and the development of the cytoskeletal network, accelerating neurotoxicity. Arsenic can also associate with molecules including dopamine, leading to an increase in circulating Lewy bodies. (Abdul et al., 2015)( Prakash et al., 2016)(Thakur et al., 2021)(Tyler & Allan, 2014)(created on BioRender.com).**

Studies on the mechanisms of arsenic-induced toxicity have established that arsenic alters learning and memory in behavioural assays and impacts multiple neurobiological processes including those of neurogenesis and cholinergic, glutamatergic, and monoaminergic signalling pathways. Recent work using animal models has revealed potent alterations in hippocampal function, morphology, and signalling leading to altered cognitive behaviour after arsenic exposure (Tyler & Allan, 2014). In a case control study, increased urinary arsenic excretion in patients was observed in correlation with enhanced risk of progression of Alzheimer's disease (AD). AD is a progressive neurological disorder characterized by the formation of neurofibrillary tangles and  $\beta$ -amyloid ( $A\beta$ ) plaques (Thakur et al., 2021). Chronic exposure to arsenic in rats caused behavioural deficits which were associated with high levels of amyloid-  $\beta$ , increased advanced glycation-end products and  $\beta$ -secretase (BACE-1) activity in the brain (Thakur et al., 2021).

Arsenic exacerbated amyloid- $\beta$  and phosphorylated tau in transgenic AD rodent models, which were mediated through bioenergetic dysfunction and modified redox metabolism (Thakur et al., 2021). Arsenic toxicity may also synergize with dopamine to cause neurotoxicity, and cause  $\alpha$ -synuclein aggregation, which is a hallmark of Parkinson's disease (Thakur et al., 2021). Few studies also provide evidence of depletion of GSH and other antioxidant enzymes in arsenic toxicity leading to mitochondrial impairment and exposing the cells to oxidative damage (Prakash et al., 2016). Lastly, the most important mechanism involved in arsenic induced neurotoxicity is the disorganisation of cytoskeletal framework either by altering protein composition of cytoskeleton and/or hyper-phosphorylation of

proteins. Further, arsenic is also capable of inducing neuronal apoptosis via activation of p38 and c-Jun N-terminal kinase-3 (JNK3) mitogen-activated protein kinases (Abdul et al., 2015).

### 2.3.5 Iron

Iron is used for several crucial metabolic functions. It is stored within cytosolic ferritin, or exported from the cell via FPN1. Cellular iron concentrations are modulated by the iron regulatory proteins (IRPs) IRP1 and IRP2 (Anderson & Frazer, 2017). The fraction of iron absorbed from the amount ingested is typically low but may range from 5% to 35% depending on circumstances and type of iron. Iron absorption occurs by the enterocytes by divalent metal transporter 1, a member of the solute carrier group of membrane transport proteins. This takes place predominantly in the duodenum and upper jejunum (Abbaspour et al., 2014). Almost two-thirds of the body iron is found in the haemoglobin present in circulating erythrocytes, 25% is contained in a readily mobilizable iron store, and the remaining 15% is bound to myoglobin in muscle tissue and in a variety of enzymes involved in the oxidative metabolism and many other cell functions (Abbaspour et al., 2014).

Under normal physiologic conditions, body iron amounts range from 3 to 5g (Anderson & Frazer, 2017). Iron levels in the brain and body increase sharply up to 30 years of age due to a metabolic need during the growth process and remain stable during adulthood, where region-specific increases in total iron is observed (Ndayisaba et al., 2019). Competition studies suggest that several other heavy metals may share the iron intestinal absorption pathway including lead, manganese, cobalt, and zinc (Abbaspour et al., 2014). In the diet, iron is either sequestered within heme or in various nonheme forms. Nonheme iron is transported across the apical membrane of the intestinal enterocyte by divalent metal-ion transporter 1 (DMT1) and is exported into the circulation via ferroportin 1 (FPN1). Newly absorbed iron binds to plasma transferrin and is distributed around the body to sites of utilization with the erythroid marrow having particularly high iron requirements (Anderson & Frazer, 2017).

Ferritin is the major intracellular iron-storage protein. Small amounts of ferritin are secreted from the cell, and the amount that is secreted strongly correlates with the concentration of intracellular iron (Anderson & Frazer, 2017). Concentrations of the ferritin protein have been reported in the substantia nigra of PD patients and also in cases of incidental Lewy body disease (Dusek et al., 2015).

The highest iron levels are observed in the basal ganglia. In addition, iron accumulation varies among brain cell types, as neurons, micro- and astroglia accumulate iron over their lifespan (Ndayisaba et al., 2019). It has been known that iron accumulates in the basal ganglia and substantia nigra in Parkinson's disease with the resultant oxidative stress being of interest as an important potential driver of neurodegeneration (Thomas et al., 2021). Iron overload has also been associated with other genetic defects (e.g. atransferrinemia, aceruloplasminemia, and Friedreich ataxia), chronic disorders (e.g. chronic liver disease and porphyria cutanea tarda), surgery (e.g. portacaval shunting), or disease treatments (e.g. transfusion therapy for myelodysplastic syndromes). Furthermore, excess iron can influence the severity of a range of other diseases such as fatty liver disease, cystic fibrosis, and a wide range of neurologic disorders (Anderson & Frazer, 2017).

High levels of iron in the tissue cause a build-up of toxic reactive oxygen species that interfere with mitochondrial function, damage DNA, catalyse dopamine oxidation reactions to produce toxic quinones and irreversibly modify proteins through highly reactive aldehydes, all ultimately leading to cell death (Thomas et al., 2021). Figure 2-8 demonstrates the effects of excess iron or chronic iron exposure.

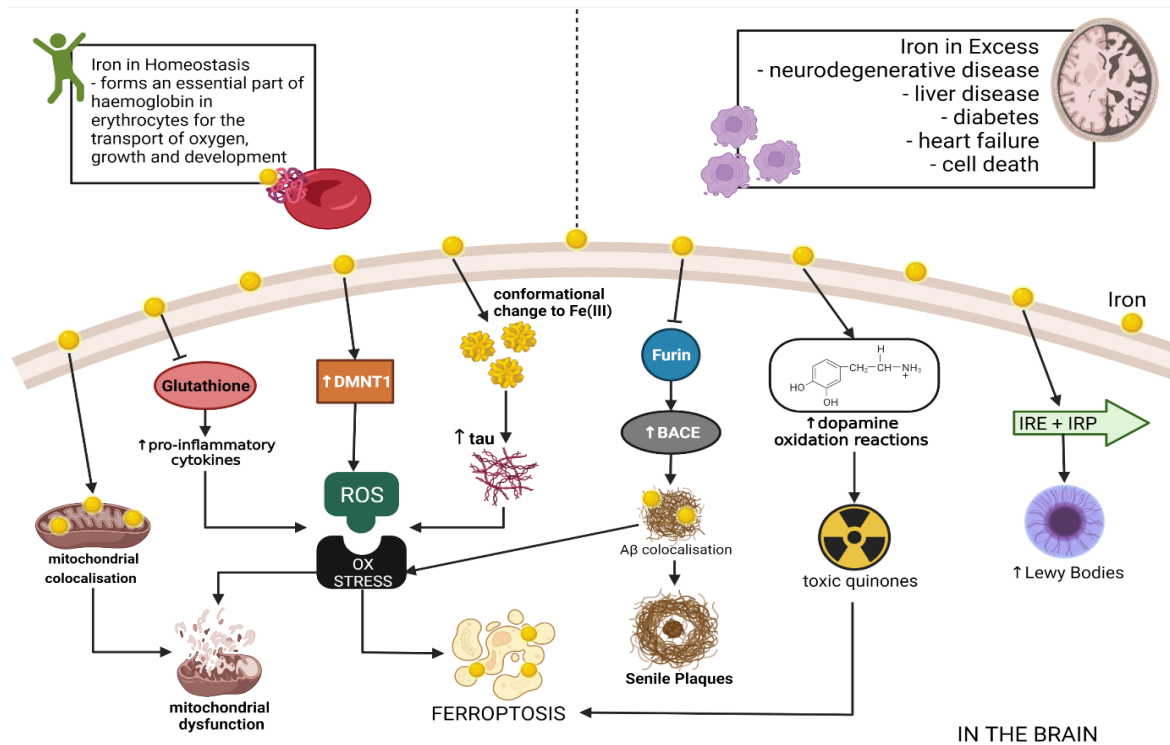


**Figure 2.8: The pathways in which dysfunction and toxicity due to excess iron, occur in the brain. In homeostatic conditions, iron plays an essential role in oxygen transportation in the bloodstream. However which chronic exposure to excess iron, the functions in the brain are dysregulated, leading to cell death through ferroptosis and the accumulation of iron-localising toxic proteins (Ndayisaba et al., 2019)(Thomas et al., 2021)(Anderson & Frazer., 2017) (created on BioRender.com).**

Iron accumulating at toxic levels within neurons, as seen in neurodegeneration, may lead to cell death via apoptosis, autophagy, necrosis or ferroptosis, a recently discovered mechanism of iron-mediated cell death distinct from apoptosis (Ndayisaba et al., 2019). Ferroptosis represents a recently discovered form of cell death independent of the caspase pathway and involves iron dysregulation, lipid peroxidation and inflammation as major hallmarks. Central to this phenomenon is the depletion of glutathione, an antioxidant that buffers ROS and binds to labile iron. Targeting ferroptosis in neurodegeneration may represent an attractive target for disease modification (Ndayisaba et al., 2019). In glial cells, iron accumulation triggers the release of pro-inflammatory cytokines, thereby creating a pro-inflammatory environment which promotes neurodegeneration (Ndayisaba et al., 2019). A large part of intracellular iron is utilized for synthesis of heme and iron-sulphur clusters in mitochondria, making iron homeostasis is heavily dependent upon proper mitochondrial function (Ndayisaba et al., 2019). Knockdown of mitoferrin-1 in an Alzheimer model of *Caenorhabditis elegans* reduces paralysis rate and slows progression of AD by decreasing mitochondrial iron accumulation and ROS generation, showing that mitochondrial iron homeostasis may substantially impact neurodegeneration (Ndayisaba et al., 2019).

Goodman et al., provided the first evidence for iron accumulation in senile plaques of post-mortem AD brains (Goodman, 1953), and more recently, brain imaging of patients with early-stage AD demonstrated increased iron concentrations co-localizing with A $\beta$  plaques which may both promote disease development and progression. Increased iron levels are believed to enhance A $\beta$  production via

downregulation of furin, a proprotein convertase participating in  $\alpha$ -secretase dependent APP processing, which in turn activates  $\beta$ -secretase implicated in  $A\beta$  generation (Ndayisaba et al., 2019). The IRP-IRE signalling pathway is also involved in proteostasis of APP (Ndayisaba et al., 2019).  $\alpha$ -synuclein possesses IRE and IRP complexes during iron overload increase its translation resulting in elevated total  $\alpha$ -synuclein burden (Ndayisaba et al., 2019). Whereas Fe (II) forms a reversible interaction through threonine residues, Fe (III) induces an irreversible conformational change, both of which promote aggregation of tau. Tau accumulation in tangles on the other hand leads to induction of heme-oxygenase 1, an antioxidant that promotes release of the redox-active Fe(II), which releases free radicals to generate oxidative stress. This in turn promotes tau hyperphosphorylation and aggregation (Ndayisaba et al., 2019).

Excess iron also interacts directly and indirectly through free radical species with key pathological proteins associated with Parkinson's disease by promoting the aggregation of  $\alpha$ -synuclein, stimulating the production of amyloid- $\beta$  via the downregulation of furin and increasing the toxicity of amyloid- $\beta$  either directly or through increased tau phosphorylation (Thomas et al., 2021). Taken together, it becomes clear that each of the metals highlighted, engages with pathways that impact either cellular proteostasis or mitochondrial quality control, both critically linked to the molecular pathology of neurodegeneration.

## CHAPTER 3: ASSESSING CYTOTOXIC EFFECTS OF METALS

### 3.1 INTRODUCTION

To address the aims of the project, a comprehensive methodology approach, employing, molecular and biochemical techniques, cytotoxicity assessment, ICPMS-based water elemental analysis, advanced single molecular imaging and EDX analysis was used. These methods were used to quantify abundance and presence of copper, manganese, cadmium and iron, in the context of autophagy pathway intermediates based on light chain-3 (LC3), lysosomal associated membrane protein 2A (LAMP2) and protein cargo (p62/Sequestosome, NBR-1, APP and amyloid-beta). Lysosomal dysfunction was uniquely assessed by employing acidotropic trackers and a galectin-3-GFP probe.

### 3.2 SAMPLING AND SAMPLE ANALYSIS

#### 3.2.1 Study sites and water sample collection

In order to assess the elemental composition of drinking water and surface water was collected at two sites, one in Limpopo and Northern Cape provinces. In the Limpopo region, 11 samples from various sources, included municipal water, bore hole water and surface water, have been collected (Figure 3-1). In order to assess the surface and drinking water in mining regions associated with iron and manganese mining activities, 15 samples were collected in the Northern Cape, specifically in the Kathu and Postmasburg region (Figure 3-2). A complete elemental and trace elemental analysis was performed.

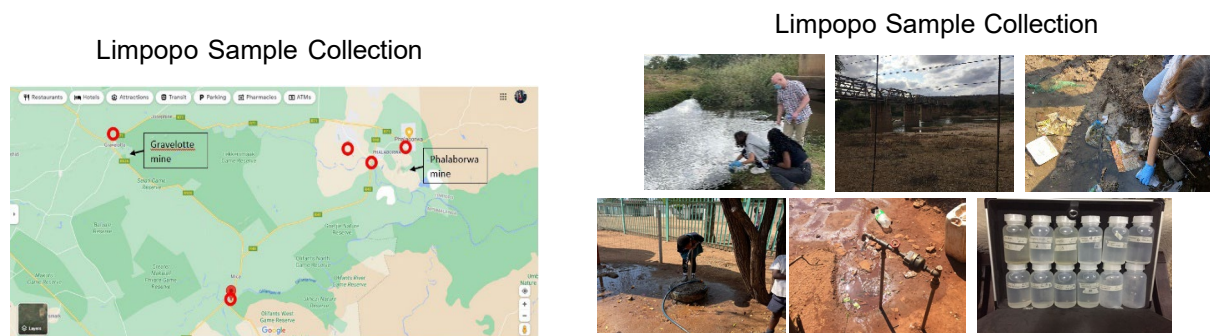


**Figure 3.1: Region of sample collection. A total of 11 samples were taken in the encircled regions of the map.**

- 1 Gamagara, Katau 1
- 2 Kathu Primary
- 2 Kathu Primary
- 3 KCS (Municipal)
- 4 Kathu High School Dam
- 5 Kathu High School Tap water
- 6 Postmasburg Surface water
- 7 Ratang Thuto Primary School PMG
- 8 Postmasburg Surface water \*\*\*
- 9 Deben Borehole near Gamagara
- 10 Deben Primary School
- 11 Hotazel Combined School
- 12 Maipeng Local Tap water
- 13 Maipeng surface H2O
- 14 Kanvo Lodge Kathu
- 15 Olifanteloop 7 Olifantehoek



Figure 3.2: Sample collection Northern Cape, including rivers, surface water and municipal water sources.

### 3.2.2 Assessing the possible cytotoxic effect of the respective metal microenvironment

#### 3.2.2.1 Proposed flow of experiments

In order to understand the impact of the respective metal exposure on neuronal toxicity, a range of analyses were employed. Specifically, cell toxicity, neuronal metal uptake, protein abundance of key markers, the autophagy and lysosome compartment and mitochondrial quality control were analysed. For all metal treatments, the WST-1 Assay was performed to measure cell proliferation, cell viability and cytotoxicity in mammalian cells. In vitro assays were used to study Amyloid Precursor Protein (APP) expression in response to exposure to metals.

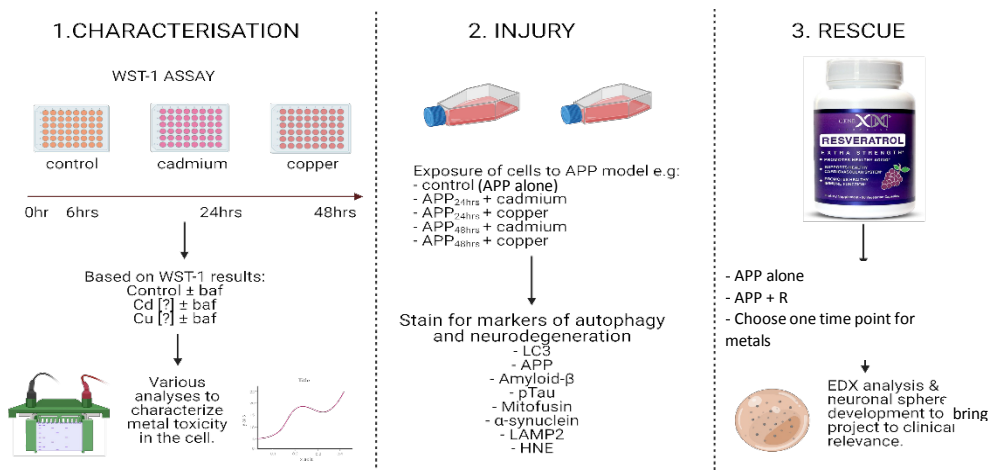


Figure 3.3: Overall scheme of experimental design and set up.

### 3.2.2.2 EDX analysis

Energy dispersive X-ray (EDX) analysis is a technique of elemental analysis associated to electron microscopy based on the generation of characteristic x-rays, revealing the abundance and localisation of elements present in a specimen. The approach allows the determination of elemental composition at subcellular levels with high quantitative accuracy and spatial resolution. Applications of EDX analysis thus far include the microanalysis of asbestos isotype characterisation, the identification of elemental composition of tissue calcification and the development of nanotechnology (Scimeca et al., 2018).

#### Sample Preparation

Wildtype N2a cells were seeded into T25 flasks for sampling. A separate flask for each metal treatment group was used, and cells were exposed to 500  $\mu\text{M}$  for copper, 500  $\mu\text{M}$  manganese, 500  $\mu\text{M}$  iron and 75  $\mu\text{M}$  for cadmium. These concentrations were used following confirmation of resultant cell viability as well as the highest concentrations having a high probability of being within the detectable limits for EDX analysis. Arsenic treatment included the highest concentration obtained in the water analysis conducted at the Gravelotte Primary school, 0.528  $\mu\text{M}$ . For cellular sample preparation, cells were dissociated, whereby following centrifugation they were resuspended in PBS and centrifuged again. Cells were then resuspended in 4% PFA and incubated for 10 min at 37°C following another centrifugation step. The cell pellet was then washed in PBS and centrifuged. The pellet was then kept in fresh PBS for transport to the CAF unit at Tygerberg medical campus, where preparation for resin embedding took place. Cell pellets were embedded in resin and sectioned at 500 nm thick sections using the Leica UC7 Ultra-Microtome and placed onto Nickel grids suitable for STEM and EDX analysis. The grids were then sent back to the CAF unit on main campus, for EDX analysis. The grids were imaged and analysed using a Zeiss MERLIN Field Emission Scanning Electron Microscope at the Electron Microbeam Unit of Stellenbosch University's Central Analytical Facility.

#### Protocol Optimisation

Protocol optimisation was required for this study due to the nature and sensitivity of the samples, a technique that offers crucial high-resolution Backscatter (BSD) images to locate an analysis point. With this technique, regions as small as 1 micron, could be identified and analysed with certainty. Prepared grids were gold coated using the Leica EM ACE200 gold coater prior to analysis. The SEM-EDX analysis technique has been in-house optimised further for cells by using natural mineral reference materials. The reference materials were obtained from Astimex, a commercial supplier of polished metallic elements, mineral standards suitable for scanning electron microscope X-ray analysis. Micro-Analysis Consultants (MAC) standards (#6409) for pyrite was used for copper, cadmium and arsenic, as well as the Astimex Scientific Limites Mineral Mount (Serial no. 03-040) standards for jadeite for iron and olivine for manganese were used for calibrating standards and verification of the analysis. The SEM-EDX analytical beam conditions for analyses of metal phases were 20 kV accelerating voltage, a working distance of 9.5 mm and a counting time of 10 live time seconds. The system is designed to performed high resolution imaging concurrently with quantitative analysis with errors ranging from  $\pm 0.6$  to 0.1 weight percentage on major elements (osmium, carbon, aluminium, magnesium, nickel and oxygen) using EDX and  $\pm 0.01$  to 0.03 weight percentage on trace elements (copper, cadmium, iron, manganese and arsenic). The physical limitations of the EDS do not allow for the analysis of elements lighter than boron.

#### Quantitative Spot Analysis

Spot analysis was performed using the Oxford INCA software, as this software enabled the use of the developed standards high-lighted in (3.5.2). Using the Zeiss Merlin 5-diode Back Scattered Electron (BSE) Detector (Zeiss NTS BSD) and Zeiss SmartSEM software, single cells were be imaged in analytical mode at a scan speed of 5, live-time of 30 secs, EHT of 20 kV and WD of 7-9.5 mm. Five

points within each cell were chosen, with the distinction of points in the nucleus and cytoplasm. Each selected point was analysed for its weight percentage of the following relevant elements: copper, cadmium, manganese, iron, arsenic, osmium, carbon, aluminium, magnesium, nickel and oxygen. A total of 5 cells per treatment group were used and their average weight percentage was taken for statistical analysis.

### EDX Mapping Analysis

The mapping analysis was performed using Aztec software, with the Zeiss Merlin 5-diode Back Scattered Electron (BSE) Detector (Zeiss NTS BSD) in STEM detection mode (aSTEM4A) at a resolution of 2048\*1536. Copper and iron treatment groups were chosen for the mapping analysis. Individual cells with promising representative morphology would be isolated and qualitative visualisation for the intracellular metal content was mapped with an average of 3 frames and pixel dwell time of 200, resulting in an overlay map acquired in approx. 33 minutes.

## 3.3 RESULTS AND DISCUSSION

### 3.3.1 Metal concentration profile of water samples collected

In order to assess the elemental composition of drinking water and surface water in the Limpopo province, 11 samples from various sources, included municipal water, bore hole water and surface water, were collected. A complete elemental and trace elemental analysis was performed. The results reveal particularly high levels (above the allowable limit) of manganese, iron, copper and arsenic. However, cadmium was below the detectable limit (Table 3.1). Table 3.2 shows the metal composition of the samples collected in the Northern Cape. Of concern is the surface/river water composition (Namagale stream and Ga-Selati river) as well as the borehole at the Gravelotte Primary school. These results were taken into consideration when implementing the experimental design. For some of the data, such as the arsenic, the exact same conditions have been re-created *in vitro*.

**Table 3.1: LCPMS analysis of 11 samples collected in the Limpopo region.**

	B	Al	V	Cr	Mn	Fe	Co	Ni	Cu	Zn	As	Se	Sr	Mo	Cd
	ug/l														
<b>LOQ</b>	<b>2,80</b>	<b>1,98</b>	<b>0,03</b>	<b>0,30</b>	<b>0,13</b>	<b>0,89</b>	<b>0,03</b>	<b>0,42</b>	<b>1,83</b>	<b>0,24</b>	<b>0,08</b>	<b>0,08</b>	<b>0,04</b>	<b>0,16</b>	<b>0,03</b>
<b>% Accuracy on internal QC</b>	<b>106</b>	<b>112</b>	<b>102</b>	<b>103</b>	<b>99</b>	<b>106</b>	<b>105</b>	<b>105</b>	<b>107</b>	<b>107</b>	<b>107</b>	<b>105</b>	<b>102</b>	<b>103</b>	<b>105</b>
Sample 1: Ga-Selati River	630,3	6314,9	38,2	24,5	192,1	4770,1	BDL	45,5	43,5	BDL	3,9	BDL	1552,2	7,1	BDL
Sample 2: Olifants River	142,1	487,0	22,2	10,8	12,9	463,7	BDL	1,5	18,8	BDL	4,5	BDL	506,3	BDL	BDL
Sample 3: Namagale stream	863,6	10441,4	56,7	54,3	207,8	8726,6	3,6	108,4	78,5	206,0	2,0	BDL	1724,1	6,0	BDL
Sample 4: Namagale Primary	169,6	185,9	22,1	7,0	BDL	137,7	BDL	4,4	98,3	BDL	3,4	BDL	659,9	0,4	BDL
Sample 5: Namagale house	149,1	352,4	20,7	6,1	BDL	182,5	BDL	3,7	BDL	BDL	2,8	BDL	643,8	BDL	BDL
Sample 6: Gravelotte Primary (borehole)	672,1	98,2	19,8	4,7	BDL	90,7	BDL	2,3	BDL	BDL	75,0	1,6	1130,9	BDL	BDL
Sample 7: Gravelotte Primary (mining)	76,4	822,8	5,2	1,9	BDL	282,7	BDL	BDL	111,8	112,7	0,3	BDL	297,5	BDL	BDL
Sample 8: Gravelotte town	171,0	676,1	5,1	7,5	1,1	322,7	BDL	3,4	61,7	BDL	3,0	BDL	333,7	BDL	BDL
Sample 9: Gravelotte shop (mining)	64,9	1311,2	3,7	14,9	BDL	171,6	BDL	13,1	76,5	33,5	BDL	BDL	300,4	BDL	BDL
Sample 10: Royal Game Guesthouse	88,1	191,7	16,7	1,9	7,2	135,2	BDL	BDL	458,6	86,2	2,0	BDL	471,6	BDL	BDL
Sample 11: TVET College Phalaborwa	123,2	216,0	19,9	4,6	2,0	139,1	BDL	2,3	168,4	51,8	2,7	BDL	593,7	BDL	BDL

**Table 3.2: LCPMS analysis of samples collected in the Northern Cape.**

	Na	Mg	Si	K	Ca	P		B	Al	V	Cr	Mn	Fe	Co
	mg/l	mg/l	mg/l	mg/l	mg/l	mg/l		ug/l						
<b>LOQ</b>	<b>0,045</b>	<b>0,001</b>	<b>1,844</b>	<b>0,126</b>	<b>0,004</b>	<b>0,024</b>		<b>1,783</b>	<b>1,139</b>	<b>0,009</b>	<b>0,069</b>	<b>0,085</b>	<b>1,773</b>	<b>0,023</b>
% Accuracy on internal QC	112	116	107	109	107	92		106	115	103	104	92	112	104
1. Gamagara, Kathu 1	32,68	7,01	25,44	21,45	39,72	0,15		41,47	14060,26	27,22	23,22	180,15	24500,44	2,03
2. Kathu Primary	24,97	52,02	14,34	2,74	84,75	<LOQ		79,10	155,19	2,11	2,03	1,84	113,30	0,30
3 Kathu Primary	25,00	51,12	14,95	2,75	86,34	<LOQ		86,73	161,08	2,25	2,02	1,86	112,66	0,29
4 KCS (Municipal)	24,42	50,92	14,94	2,76	84,05	<LOQ		74,17	110,23	2,28	1,63	0,96	63,17	0,17
5. Kathu High School Dam	22,34	48,26	15,35	2,85	82,92	<LOQ		73,07	41,32	2,37	1,24	4,35	206,22	0,19
6. Kathu High School Tap water	24,80	51,34	14,72	2,73	84,24	<LOQ		83,61	238,64	2,26	0,92	8,13	82,75	0,17
7. Postmasburg Surface water	144,35	162,12	5,19	25,98	108,31	0,29		272,94	467,96	5,19	4,26	94,19	840,12	0,67
8. Ratang Thuto Primary School PMG	32,66	65,41	18,93	3,24	100,79	0,04		97,59	27,86	2,53	1,96	1,01	84,72	0,11
9. Postmasburg Surface water ***	86,27	101,48	16,54	12,85	110,28	0,16		191,99	60,51	3,32	0,94	10,53	113,78	0,64
10. Deben Borehole near Gamagara	23,64	66,73	29,20	3,44	102,47	<LOQ		116,11	27,16	18,53	0,61	0,95	51,66	0,12
11. Deben Primary School	38,11	89,12	29,84	4,82	128,50	0,06		141,51	20,77	12,46	0,76	1,63	69,36	0,07
12. Hotazel Combined School	21,27	59,89	17,02	3,09	93,84	0,02		102,89	34,33	2,56	1,68	1,69	59,29	0,21
13. Maipeng Local Tap water	18,11	55,08	16,11	2,34	77,52	<LOQ		58,87	34,47	1,04	0,73	0,65	62,24	0,09
14. Maipeng surface H2O	0,37	3,74	13,67	4,39	29,80	0,25		35,06	5727,31	16,38	9,98	114,25	5070,04	1,91
15. Kanvo Lodge Kathu	20,69	46,01	12,87	2,55	61,34	<LOQ		82,77	67,71	1,45	1,77	1,17	87,12	0,35
16. Olifanteloop 7 Olifantehoek	5,48	3,33	14,54	2,62	5,70	0,10		20,09	5558,68	11,01	9,14	41,34	4367,09	1,38

**3.3.2 Health risk assessment**

The results reveal that the surface water is of primary concern, with values for particularly aluminium, manganese and iron being above the maximum allowable limits stated in SANS 241. When performing a health risk and hazard analysis, it becomes evident that a general health risk exists when consuming water from the Gamagara river (Table 3.3). Furthermore, the results revealed that the arsenic levels observed have detrimental health effects (Table 3.4). Due to the specific sample, collected from a borehole at a primary school (Gravelotte), feedback to the school was provided in Sept 2022 (Figure 3.4). Indeed, the school principal indicated concern, as the children had complained about stomach aches, especially in the hot summer months. Actions were taken and respective signs were installed, prohibiting consumption for drinking. The school principal indicated gratitude and thanks.

**Table 3.3: Health risk and hazard quotient analysis.**

SAMPLE NAME	Drinking Hazard Quotient			SUM
	Cu	Mn	Fe	
	HQ > 1 = RISK			
1. Gamagara, Kathu	0,013167	0,220908	2,333375	2,56745
2. Kathu Primary	0,033616	0,002253	0,010791	0,04666
3 Kathu Primary	0,033569	0,002284	0,01073	0,046583
4 KCS (Municipal)	0,040025	0,001172	0,006016	0,047213
5. Kathu High School Dam	0,007277	0,005328	0,01964	0,032245
6. Kathu High School Tap water	0,019988	0,00997	0,007881	0,037838
7. Postmasburg Surface water	0,006303	0,115494	0,080011	0,201809
8. Ratang Thuto Primary School PMG	0,018654	0,001244	0,008068	0,027966
9. Postmasburg Surface water ***	0,005215	0,012908	0,010836	0,028958
10. Deben Borehole near Gamagara	0,034365	0,00117	0,00492	0,040455

11. Deben Primary School	0,004241	0,001993	0,006606	<b>0,01284</b>
12. Hotazel Combined School	0,014773	0,002077	0,005647	<b>0,022497</b>
13. Maipeng Local Tap water	0,004482	0,000801	0,005927	<b>0,011209</b>
14. Maipeng surface H2O	0,007942	0,140102	0,482861	<b>0,630905</b>
15. Kanvo Lodge Kathu	0,10231	0,001434	0,008298	<b>0,112042</b>
16. Olifanteloop 7 Olifantehoek	0,007102	0,050694	0,415913	<b>0,473709</b>

Table 3.4: Health quotient assessment.

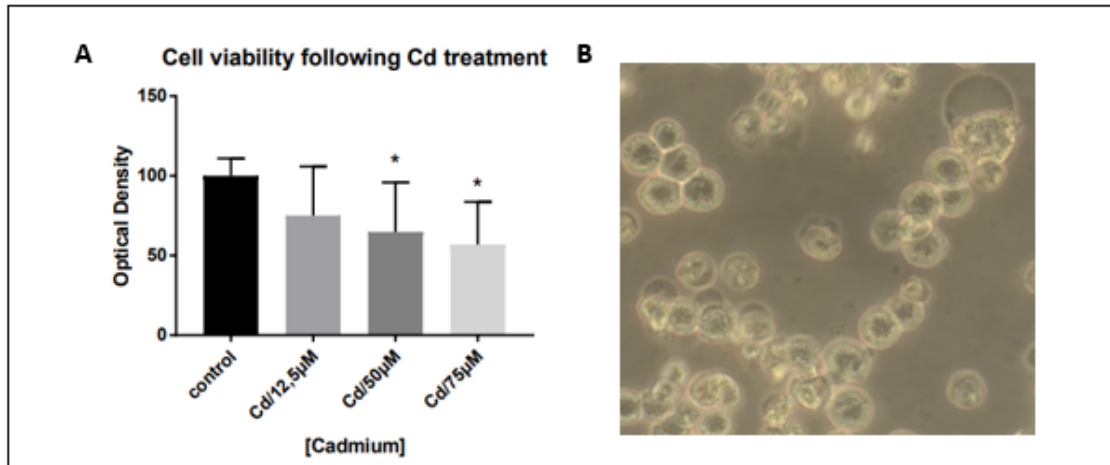
Sample number	Metal	RfD (mg/kg-d)	ICPMS concentration (mg/L)	ADD	Health Quotient (HQ)
3	Manganese	$2.33 \times 10^{-2}$	0.2078	$5.937 \times 10^{-3}$	$2.548 \times 10^{-5}$
3	Iron	$3 \times 10^{-1}$	8.7266	0.24933	$8.311 \times 10^{-3}$
6	Arsenic	$3 \times 10^{-4}$	0.075	$2.14 \times 10^{-3}$	7.13



Figure 3.4: Feedback Gravelotte primary school, Sept 2022.

### 3.3.3 Assessing the possible cytotoxic effect of the respective metal microenvironment

Next, in order to assess the possible cytotoxic effect of the respective metal microenvironment, a WST-1 assay was performed. In Figure 3.5A, it can be seen that the treatment of 75  $\mu\text{M}$  results in a 50% cell viability. In Figure 3.5B cells appear to be experiencing the most stress out of the five treatment groups, with low confluency, severe cell clumping and almost no adherence.



**Figure 3.5: A - WST-1 assay conducted using increasing Cd concentrations (12,5µM, 50 µM, and 75µM) over 24 hours. B – Microscope image of treated cells at a magnification of 40X, following a 24 hour treatment at a Cadmium concentration of 75 µM.**

Similarly, Figure 3.6A and B show a WST-1 assay conducted using increasing Mn concentrations (100 µM, 250 µM, and 500 µM) and the microscope image of treated cells at a magnification of 40X, following a 24 hour treatment at a Mn concentration of 500 µM. From the results obtained, it can be seen that , it can be seen that the treatment of 100 µM resulted in a 50% cell viability. However, no significant effects were observed when the concentration was increased. Figure 3.6B suggests that treatment of the cells with 500 µM resulted in 80% confluency and clumping. This may indicate a stress response of over proliferation, which may be time-dependent.

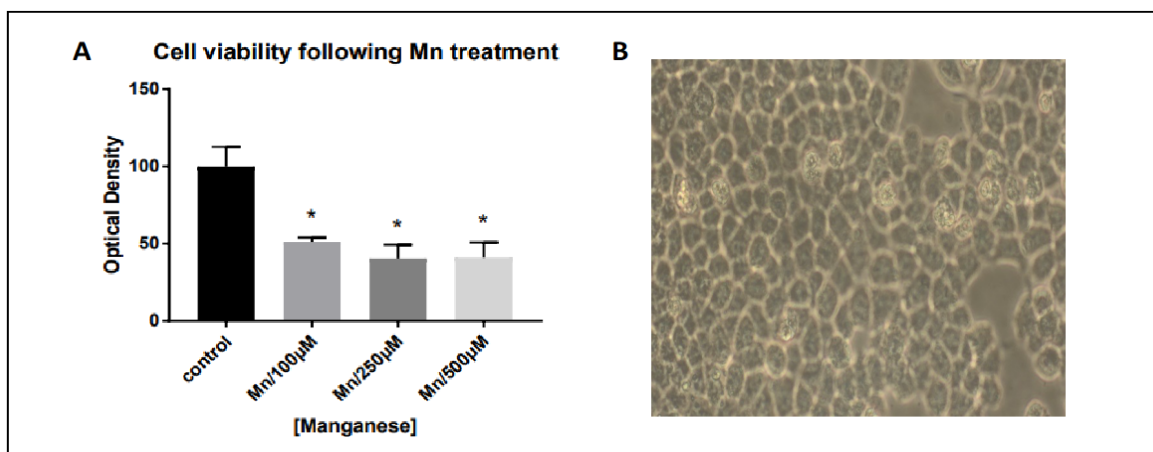
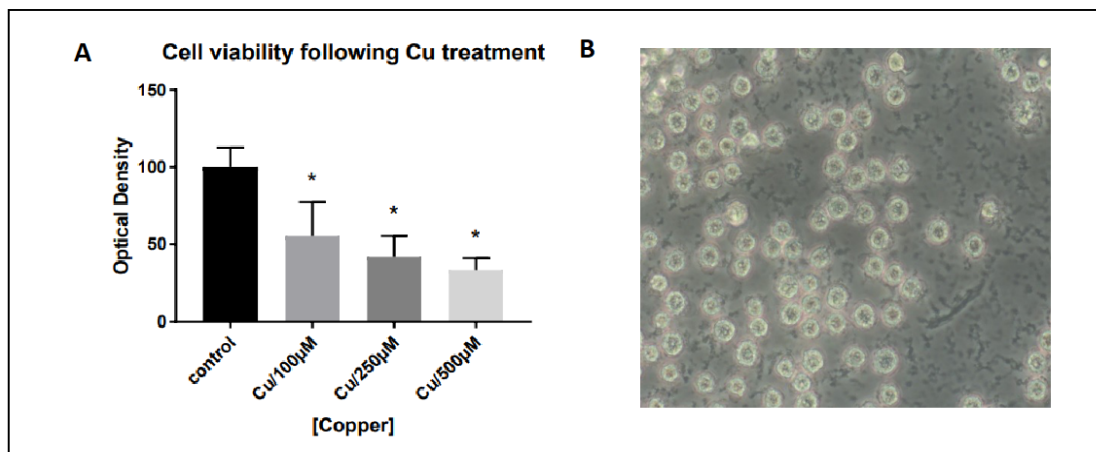


**Figure 3.6: A – WST-1 assay conducted using increasing Mn concentrations (12,5 µM, 50 µM, and 75 µM) over 24 hours. B – Microscope image of treated cells at a magnification of 40X, following a 24 hour treatment at a Mn concentration of 500 µM.**

Figure 3.7A and B show a WST-1 assay conducted using increasing Cu concentrations (100 µM, 250 µM, and 500 µM) and the microscope image of treated cells at a magnification of 40X, following a 24

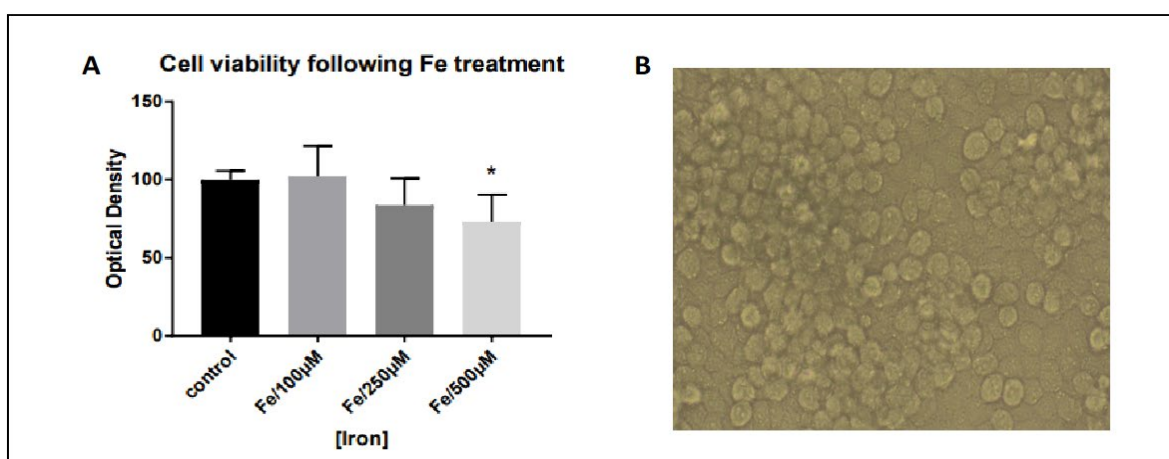
hour treatment at a Cu concentration of 500  $\mu\text{M}$ . From the results obtained, it can be seen that, it can be seen that the treatment of 100  $\mu\text{M}$  resulted in a 50% cell viability.

In Figure 3.7B the cells appear to be under stress, with little adherence and low confluency. This is in line with the WST-1 results, which indicate a significant decrease in viability with increasing Cu concentrations.



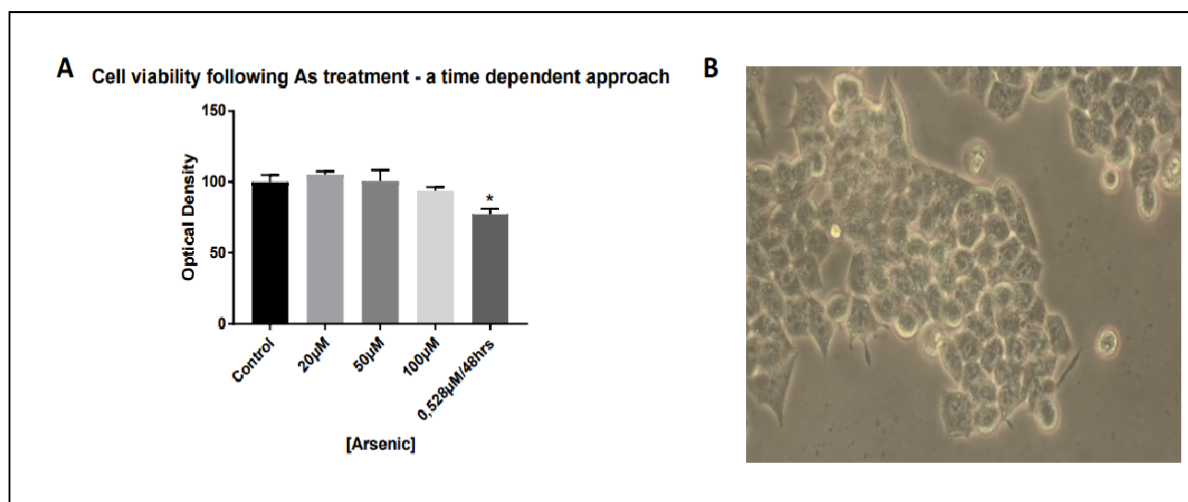
**Figure 3.7: A – WST-1 assay conducted using increasing Cu concentrations (100  $\mu\text{M}$ , 250  $\mu\text{M}$ , and 500  $\mu\text{M}$ ) over 24 hours. B – Microscope image of treated cells at a magnification of 40X, following a 24 hour treatment at a Cu concentration of 500  $\mu\text{M}$ .**

Figure 3.8A and B show a WST-1 assay conducted using increasing Fe concentrations (100  $\mu\text{M}$ , 250  $\mu\text{M}$ , and 500  $\mu\text{M}$ ) and the microscope image of treated cells at a magnification of 40X, following a 24 hour treatment at a Fe concentration of 500  $\mu\text{M}$ . From the results obtained, it can be seen that there was less decrease in cell viability (Figure 3.8A) compared to other metals. In Figure 3.8B the cells appear to be overly confluent, with extensive clumping. In accordance with the WST-1 result, this extreme confluence may indicate increase in proliferation, which may be a stress response to metal treatment.



**Figure 3.8: A – WST-1 assay conducted using increasing Fe concentrations (100  $\mu\text{M}$ , 250  $\mu\text{M}$ , and 500  $\mu\text{M}$ ) over 24 hours. B – Microscope image of treated cells at a magnification of 40X, following a 24 hour treatment at a Fe concentration of 500  $\mu\text{M}$ .**

Figure 3.9A and B show a WST-1 assay conducted using increasing As concentrations (20-100  $\mu\text{M}$ ) over 24 and 48 hours, and the microscope image of treated cells at a magnification of 40X, following a 24 hour treatment at a Fe concentration of 20  $\mu\text{M}$ . A time-dependent approach was taken for As due to its low concentrations not showing any significant effect on cell viability over 24 hours. The concentration used for the 48 hour exposure was replicated from that found in the water samples collected. The results indicated that the effect of As on the cells is not dependent on time.



**Figure 3.9: A – WST-1 assay conducted using increasing As concentrations (20-100  $\mu\text{M}$ ) over 24 and 48 hours. B – Microscope image of treated cells at a magnification of 40X, following a 24 hour treatment at an As concentration of 20  $\mu\text{M}$ .**

Overall, the results indicate and confirm the specific concentration of Cu, Cd, Mn and Fe which leads to cytotoxic effects. This information is important for subsequent in vitro analyses. Of note, As which has been utilised in a similar concentration as found in the water sample, also has cytotoxic effects, however only reaching significance upon 48 hrs of exposure.

### 3.3.4 Assessing the intracellular uptake of the metals

In this section, the intracellular uptake of the metals of interest was assessed. First, the method had to be optimised as this is the first time a study like this is performed in South Africa. Figure 3.10 provides a snapshot of the scope of work for optimisation of the protocol for EDX analysis.

For the EDX analysis, 2 distinct approaches were followed. INCA-based spot analysis was performed, to enable quantification of the element throughout the cell, while mapping was employed to visualize their intracellular distribution. Prior to image acquisition, cells were pelleted, embedded for electron microscopy, sectioned using ultramicrotomy and placed onto copper grids for subsequent acquisition and analysis. The backscatter detector was used to locate cells on the grid.

## EDX analysis – Novel Protocol Optimisation

### Energy-dispersive X-ray with Correlative Light Electron Microscopy

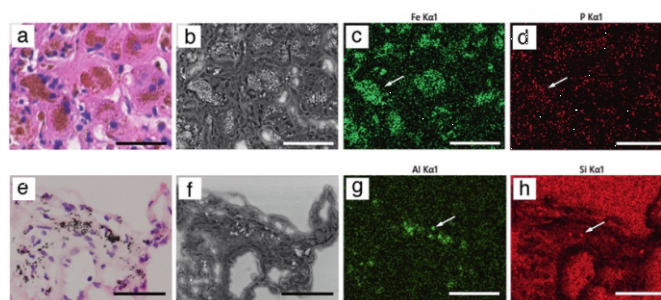
X-rays produce chemical information: the energy transferred to the atomic electron knocks it off, leaving behind a hole.

Its position is then filled by another electron from a higher energy shell, and the characteristic X-ray is released.

Chemical information can be visualized AKA identify each element that exists in the sample.

#### Aim:

We wish to quantify the abundance of copper and cadmium in relation to other metals in the cells – attempt to identify the localisation of the metals, whether they are accumulating and with rescue, can resveratrol decrease these levels or will redistribution occur?



(Lutz *et al.*, 2014)

**Figure 3.10: EDX analysis protocol optimisation, to assess the metal elemental profile in neuronal cells.**

Figures 3.11 to 3.16 show representative EDX analyses using spot quantification, showing average intracellular uptake of all metals of interest. All treated cells reveal ultrastructural hallmarks associated with damage, such as vacuole formation. Our results reveal a significant increase only in intracellular Fe concentration.

The results reveal metal-induced neuronal toxicity, with a metal-specific intracellular uptake profile. Although all metals induced neuronal toxicity and a loss in cell viability, only iron levels were significantly increased, suggesting distinct and specific uptake dynamics.

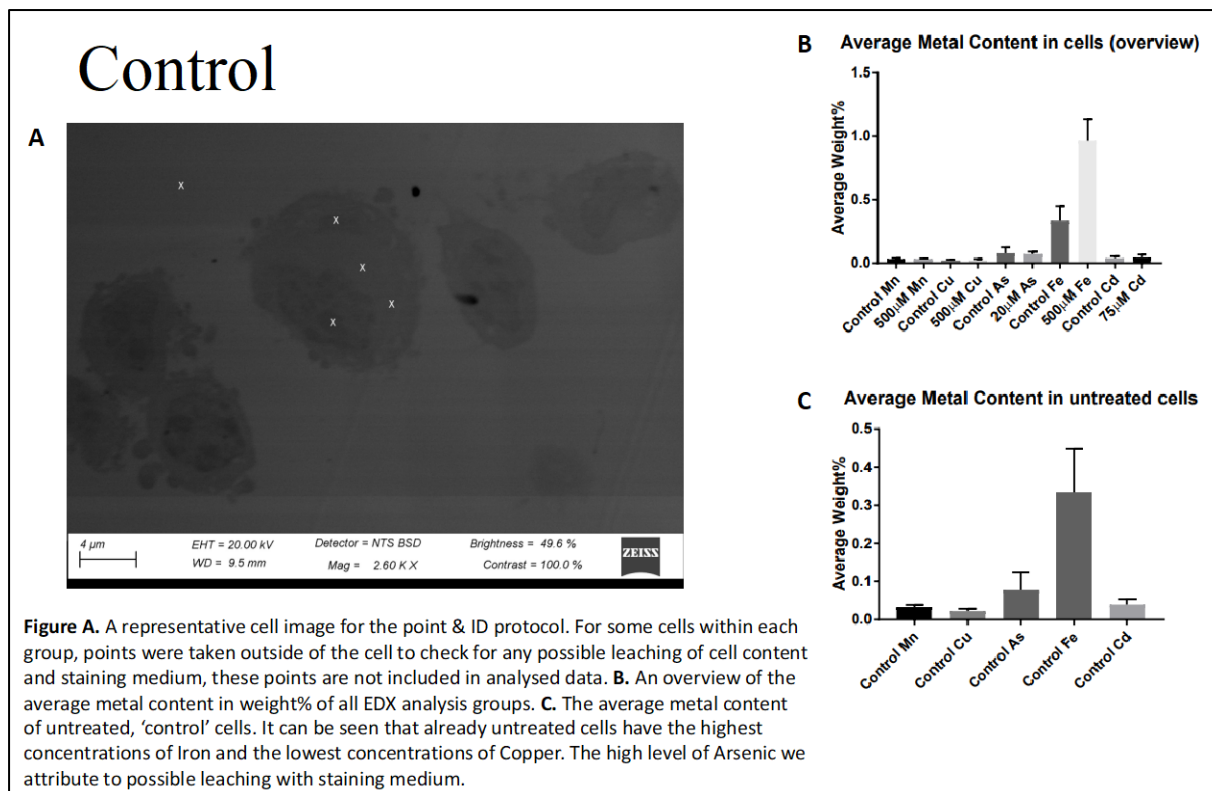


**Figure 3.11: A representative (control) EDX analysis using spot quantification, showing average intracellular uptake of all metals of interest.**

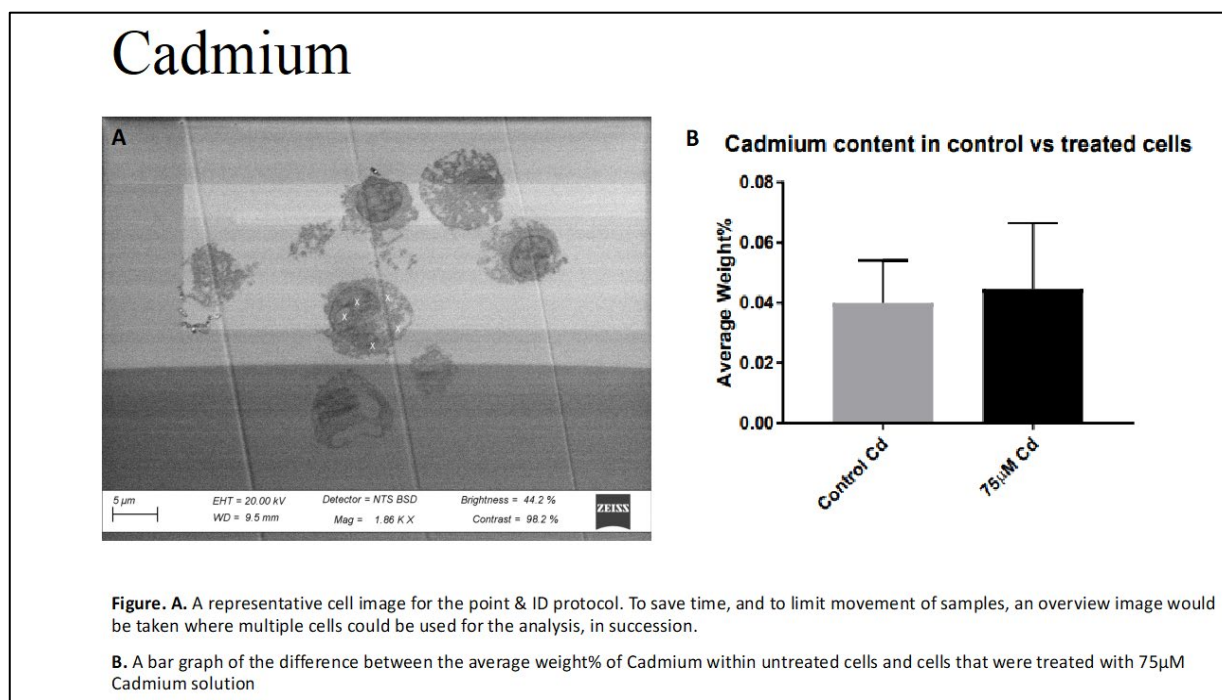
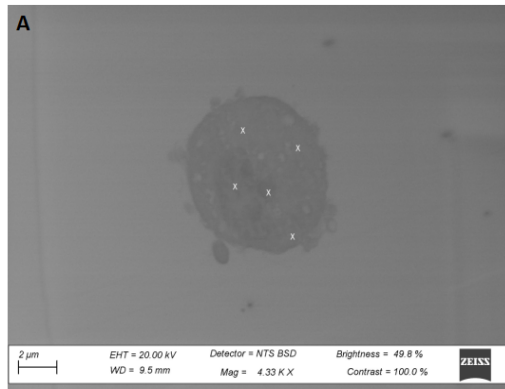


**Figure 3.12: A representative EDX analysis using spot quantification, showing average intracellular uptake of Cd.**

## Manganese



**B Manganese content in control vs. treated cells**

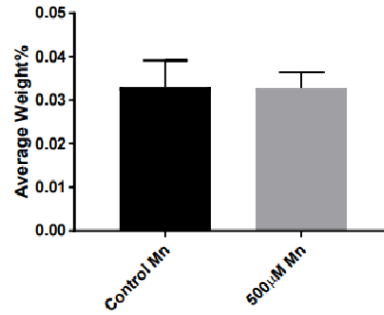
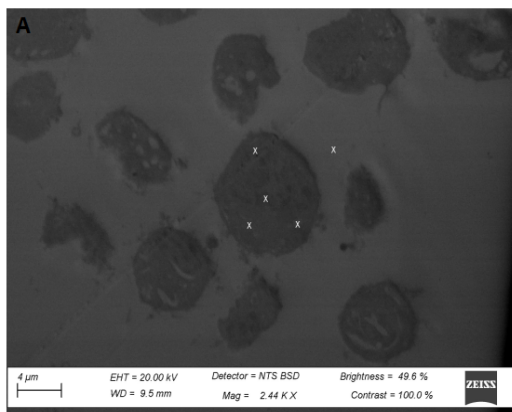


**Figure. A.** A representative cell image for the point & ID protocol.

**B.** A bar graph of the difference between the average weight% of Manganese within untreated cells and cells that were treated with 500 μM Manganese solution.

**Figure 3.13: A representative EDX analysis using spot quantification, showing average intracellular uptake of Mn.**

## Arsenic



**B Arsenic content in control vs. treated cells**

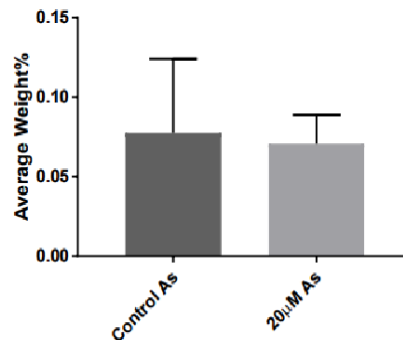


**Figure. A.** A representative cell image for the point & ID protocol. For some cells within each group, points were taken outside of the cell to check for any possible leaching of cell content and staining medium, these points are not included in analysed data.

**B.** A bar graph of the difference between the average weight% of Arsenic within untreated cells and cells that were treated with 20 μM Arsenic solution.

**Figure 3.14: A representative EDX analysis using spot quantification, showing average intracellular uptake of As.**

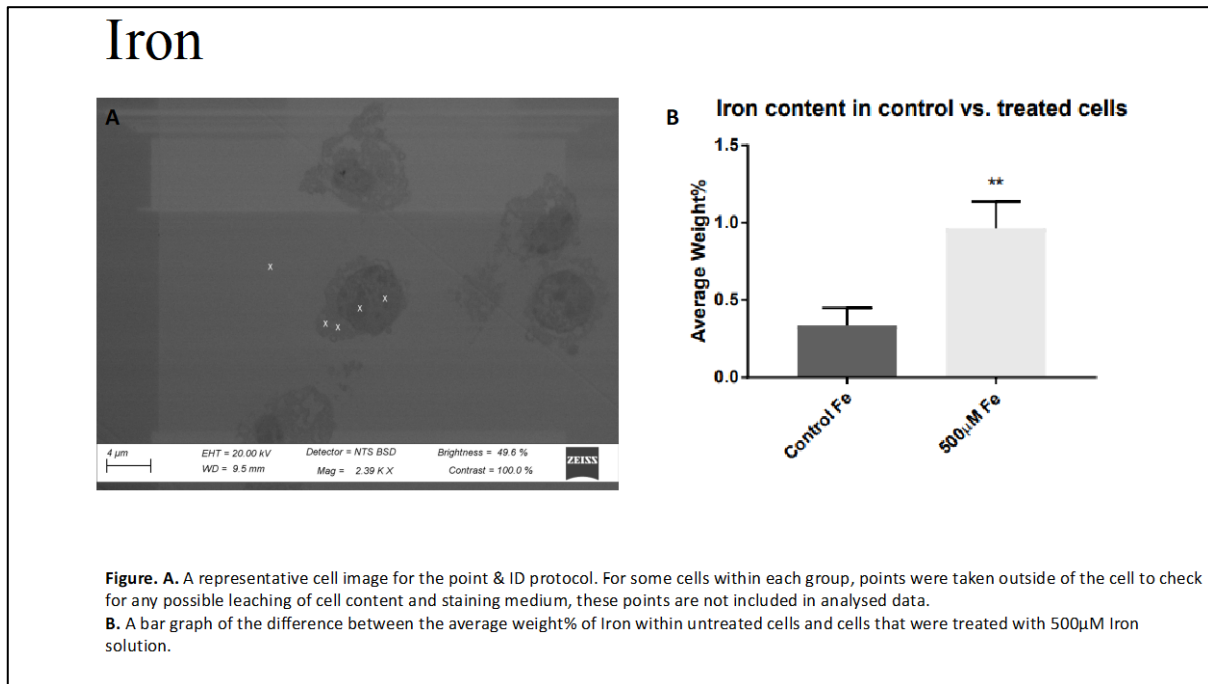


**Figure 3.15:** A representative EDX analysis using spot quantification, showing average intracellular uptake of Fe.

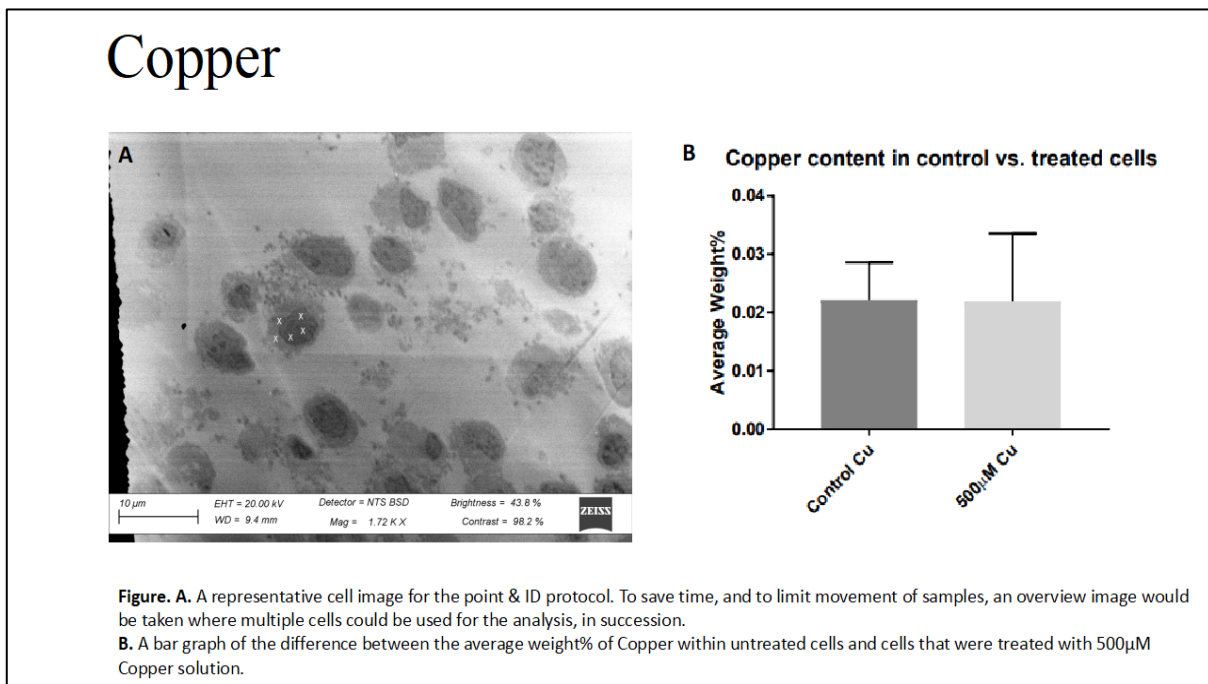


**Figure 3.16:** A representative EDX analysis using spot quantification, showing average intracellular uptake of Cu.

### 3.3.5 Assessing the impact of metal exposure

Following the EDX analysis of above samples, further molecular analysis was performed to assess the impact of metal exposure using electron microscopy. The scanning transmission electron microscopy (STEM) technique allows for the imaging and morphological characterisation of the cell, revealing ultrastructural details similar to those achieved in transmission electron microscopy (TEM). While cells were identified and imaged as part of the EDX spot analysis, these images lack quality due to the low resolution of the detector used for the specific technique. In order to precisely characterise the cellular ultrastructure of metal-treated cells, STEM imaging was used. Figure 3.17 shows the STEM images obtained after treatment with various metals of interest. The micrographs reveal ultrastructural changes within each metal-treated group. In the control group, the cells are characterized by a defined nucleus and nucleolus. The cell membrane is intact and organelles can be seen well. The cytoplasm also appears undisrupted. These are indicators that the control cells are in a healthy condition.

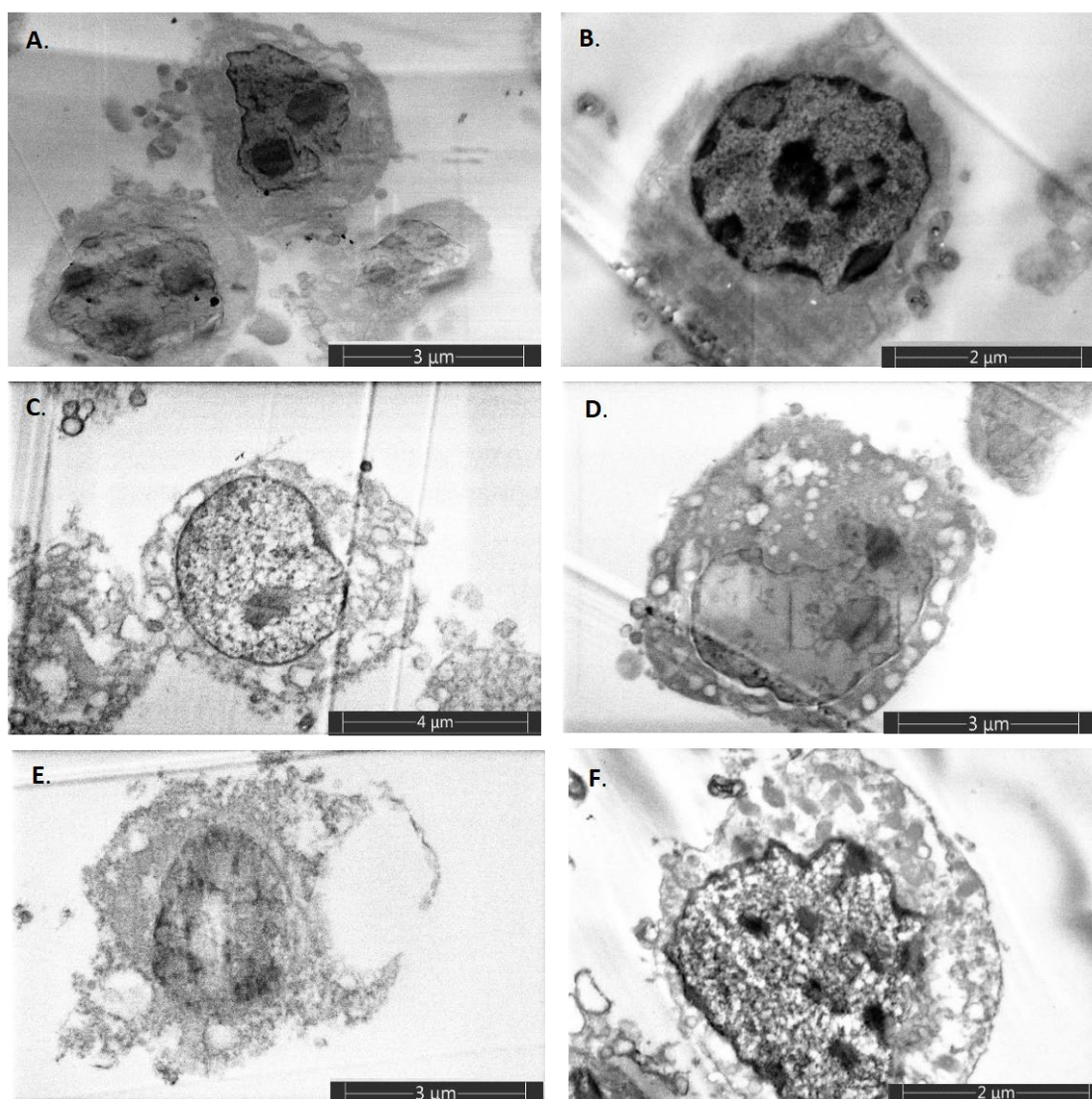


**Figure 3.17: STEM micrographs of N2a cells following various treatment. A: control cells B: exposure to 500  $\mu\text{M}$  Cu for 24 hrs. C: exposure to 500  $\mu\text{M}$  Fe for 24 hrs. D: exposure to 500  $\mu\text{M}$  Mn for 24 hrs. E: exposure to 75  $\mu\text{M}$  Cd for 24 hrs. F: exposure to 0.528  $\mu\text{M}$  As for 48 hrs. Scale bar: 2-4  $\mu\text{m}$  respectively.**

The Cu-treated cells reveal a strong difference in contrast between the nucleus and cytoplasm, an indication of copper localisation to the nucleus (Figure 3.17B). The cell membrane is however still intact. DNA fragments high in electron density, forms a horseshoe-like morphology around the nucleus. Furthermore, the nucleus is enlarged with mild chromatin condensation. The Fe-treated cells reveal an abundance of large vacuolar structures (Figure 3.17C). There is degradation of the cell membrane and cellular organelles can be poorly demarcated. The nucleus is enlarged, however there is less DNA condensation and electron dense contrast. Similarly, the Mn-treated cells present with a high abundance of vacuolar structures and cell membrane disruption (Figure 3.17D). However, the vacuolar structures appear overall smaller in size. There is also less condensation observed in the nucleus, compared to the other metal-treated groups.

Due to the poor overall condition of the Cd-treated cells, image acquisition proved to be more challenging. The cell membrane is severely disrupted and there is an indication of membrane blebbing (Figure 3.17E). Cell organelles are disintegrated, with the presence of the semblance of large vacuolar structures. The nuclear contrast is poor, suggesting that the nuclear content has also been disrupted. Finally, the As-treated cells displayed severe cellular damage (Figure 3.17F). Enlarged, electron dense nuclei can be seen. There is extensive cell membrane disintegration, with disruption of the cytosol.

### 3.3.6 Assessing primary cellular stress response

Specifically the autophagy system, as primary cellular stress response, was assessed. Here, western blotting for autophagy and lysosomal related proteins LC3 and LAMP2 was performed. The results obtained revealed that the Fe-treated cells and the As-treated cells display the highest increase in the autophagy-related proteins (Figure 3.18). In contrast, Mn-treated cells showed no difference in protein abundance overall compared to control groups, while the proteins in the Cd-treated cells were overall low in abundance.

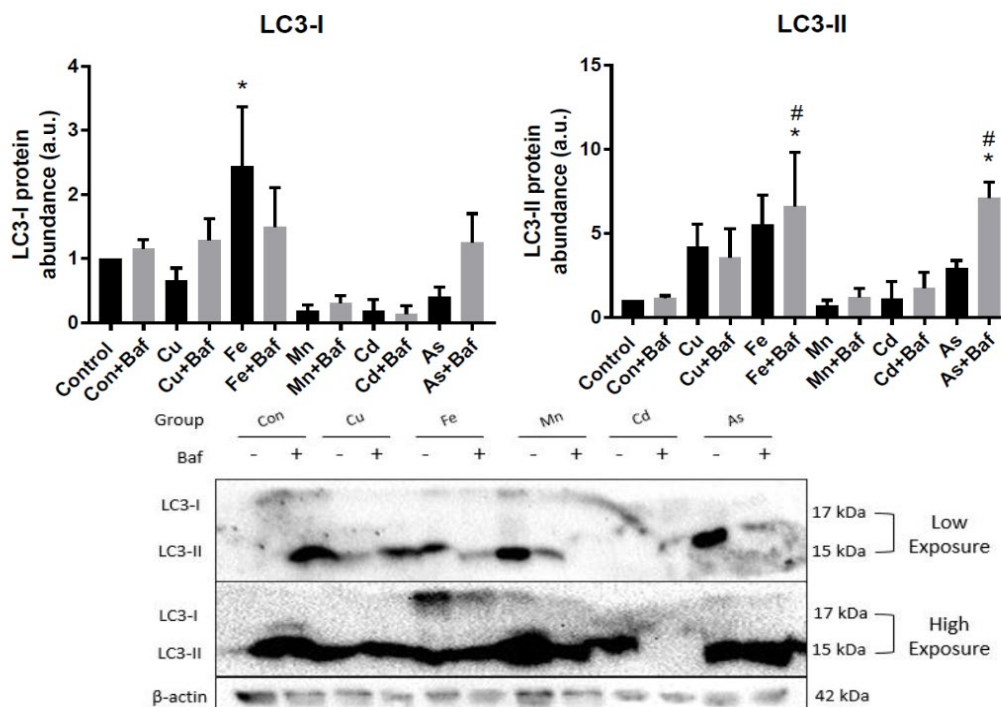


**Figure 3.18: Western blot analysis for average LC3-I and LC3-II protein abundance. Representative immunoblots for both proteins as well as  $\beta$ -actin are shown for the following groups in the absence (-) and presence (+) of 400 nM Baf: control, 500  $\mu$ M Cu, 500  $\mu$ M Fe, 500  $\mu$ M Mn, 75  $\mu$ M Cd and 0.528  $\mu$ M As. A low- and high-exposure micrograph has been provided so as to better visualise LC3-I. \* $p < 0.05$  vs Control, # $p < 0.05$  vs Con + Baf.  $n = 4$**

### 3.3.7 Assessing the extent of neuronal toxicity due to metal exposure

Next, in order to assess the extent of neuronal toxicity due to metal exposure in the context of amyloid-induced cellular injury, the transgenic APP NA2 cell line was used, and APP was overexpressed. The results obtained showed that only copper and cadmium exacerbated amyloid-induced toxicity (Figure 3.19), suggesting that these metals require specific attention in the context of neurodegeneration. The other metals, Mn and Fe, did not lead to additional cell death in the presence of amyloid beta generation.

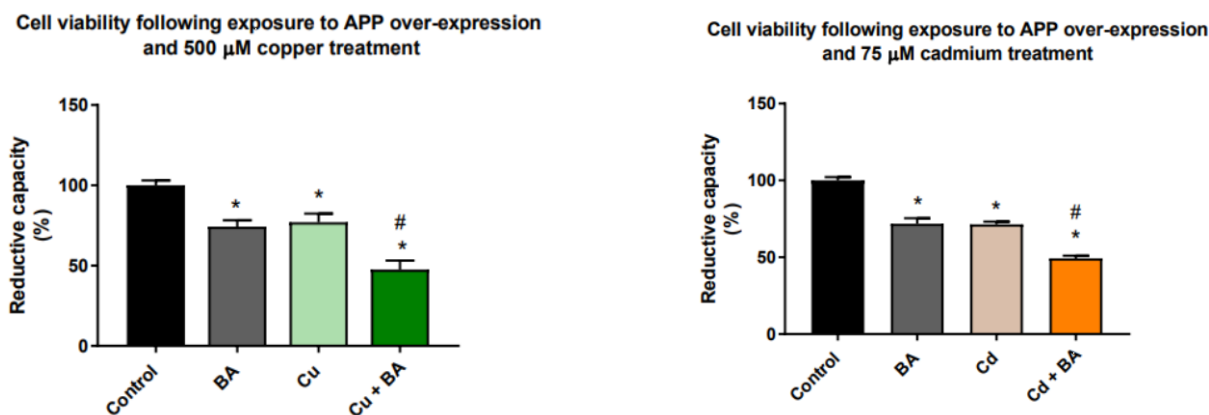


Figure 3.19: Cell viability in the presence of amyloid-induced toxicity.

### 3.3.8 Evaluating the role of the lysosomal compartment as part of the cellular stress response

Next, in order to further understand the role of the lysosomal compartment as part of the cellular stress response, particularly for the metals copper and cadmium, confocal microscopy was performed, assessing the lysosomal acidic compartment. Our results reveal a distinct response by the cells. Engaging the lysosomal compartment upon APP overexpression, with distinct responses upon copper and cadmium exposure (Figures 3.20-3.22).

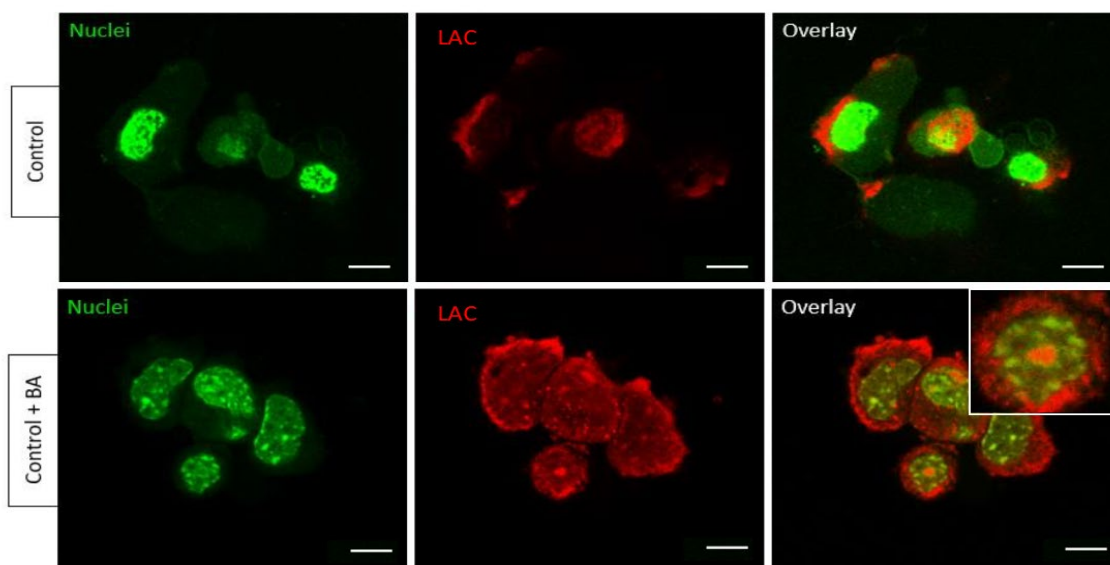


Figure 3.20: Fluorescence micrographs indicating the nuclei and lysosomal acidic compartments (LAC) of APP cells for the control experiment. Scale bar represents 10 µm. A minimum total number of 2 fields of view each were acquired for 2 independent experiments.

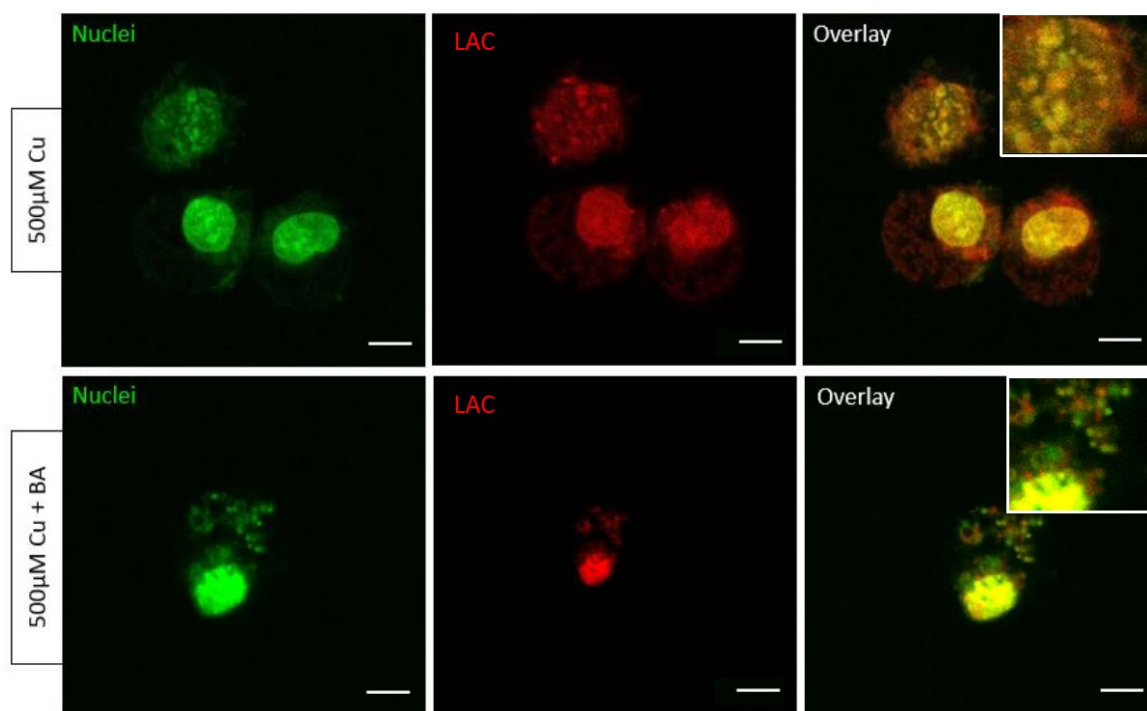


Figure 3.21: Fluorescence micrographs indicating the nuclei and lysosomal acidic compartments (LAC) of APP cells following 500  $\mu\text{M}$  Cu only treatment over 24 hours and 500  $\mu\text{M}$  Cu with 5 mM butyric acid for 6 hours using 2 mg/ml acridine orange dye. Scale bar represents 10  $\mu\text{m}$ . A minimum total number of 2 fields of view each were acquired for 2 independent experiments.

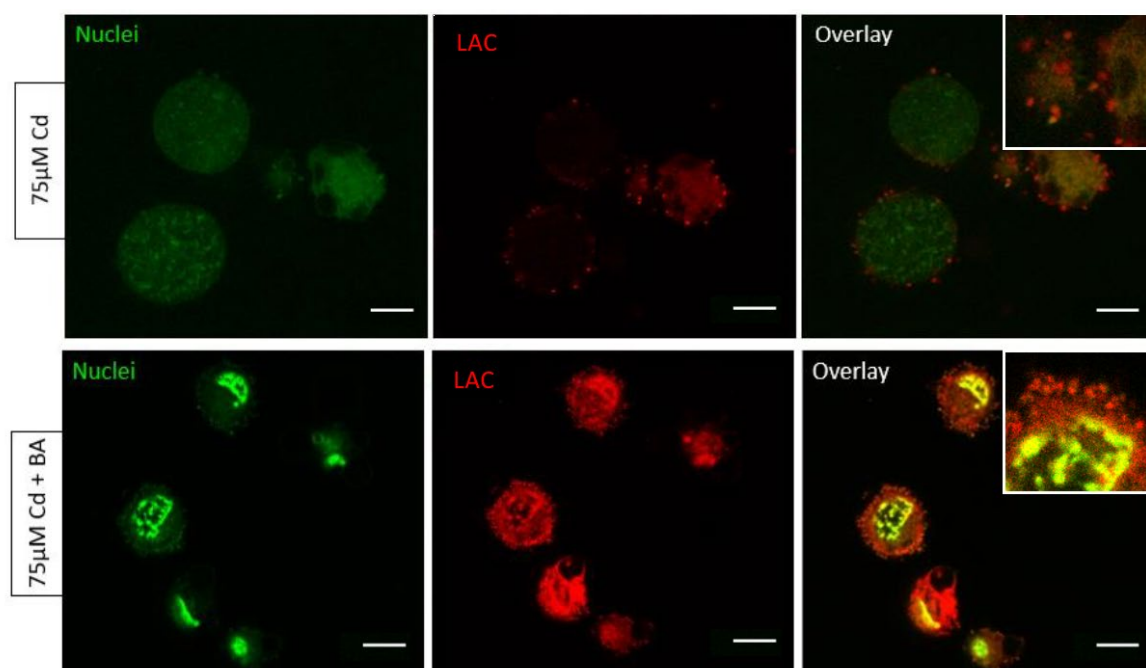


Figure 3.22: Fluorescence micrographs indicating the nuclei and lysosomal acidic compartments (LAC) of APP cells following 75  $\mu\text{M}$  Cd only treatment over 24 hours and 75  $\mu\text{M}$  Cd with 5 mM butyric acid for 6 hours using 2 mg/ml acridine orange dye. Scale bar represents 10  $\mu\text{m}$ . A minimum total number of 2 fields of view each were acquired for 2 independent experiments.

### 3.3.9 Assessing the impact of metal exposure on cell viability and proliferation

The concentrations of iron, manganese and copper were established, especially with the aim to dissect the effect of the metal exposure on cell viability and cell proliferation. The results obtained generally indicated that all of the metals assessed are toxic to the cells in a concentration dependent manner (Figure 3.23). However, lower Fe concentrations enhances cell proliferation, with only high concentrations, of about 500  $\mu\text{M}$ , resulting in a significant decrease in cell viability (Figure 3.24). Furthermore, the results indicate that the metal exposure leads to mitochondrial disruption, impacted mitochondrial fusion, especially for Cu and Mn-treated cells (Figure 3.25).

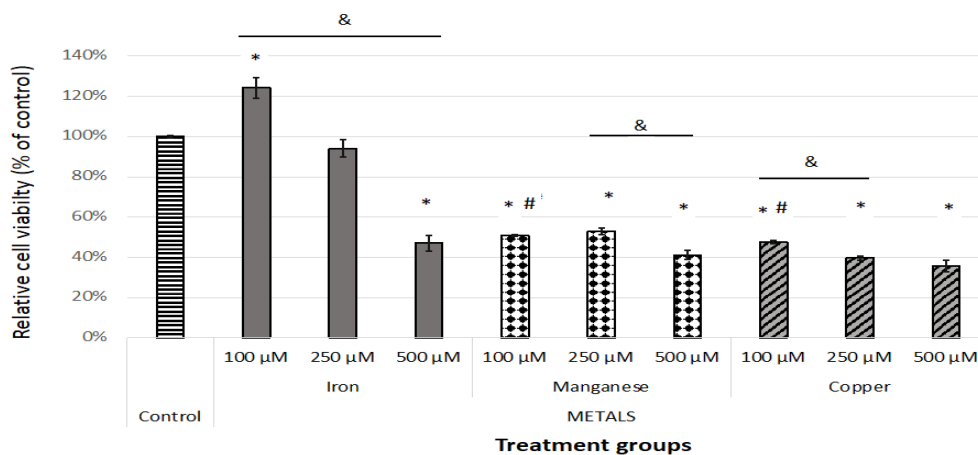


Figure 3.23: Cell viability analysis and cell count for exposure to all metals.

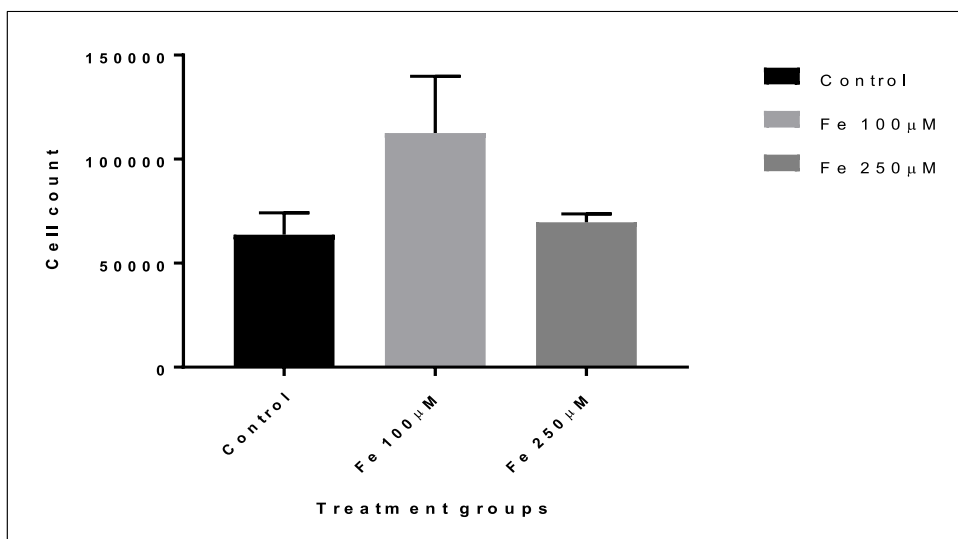
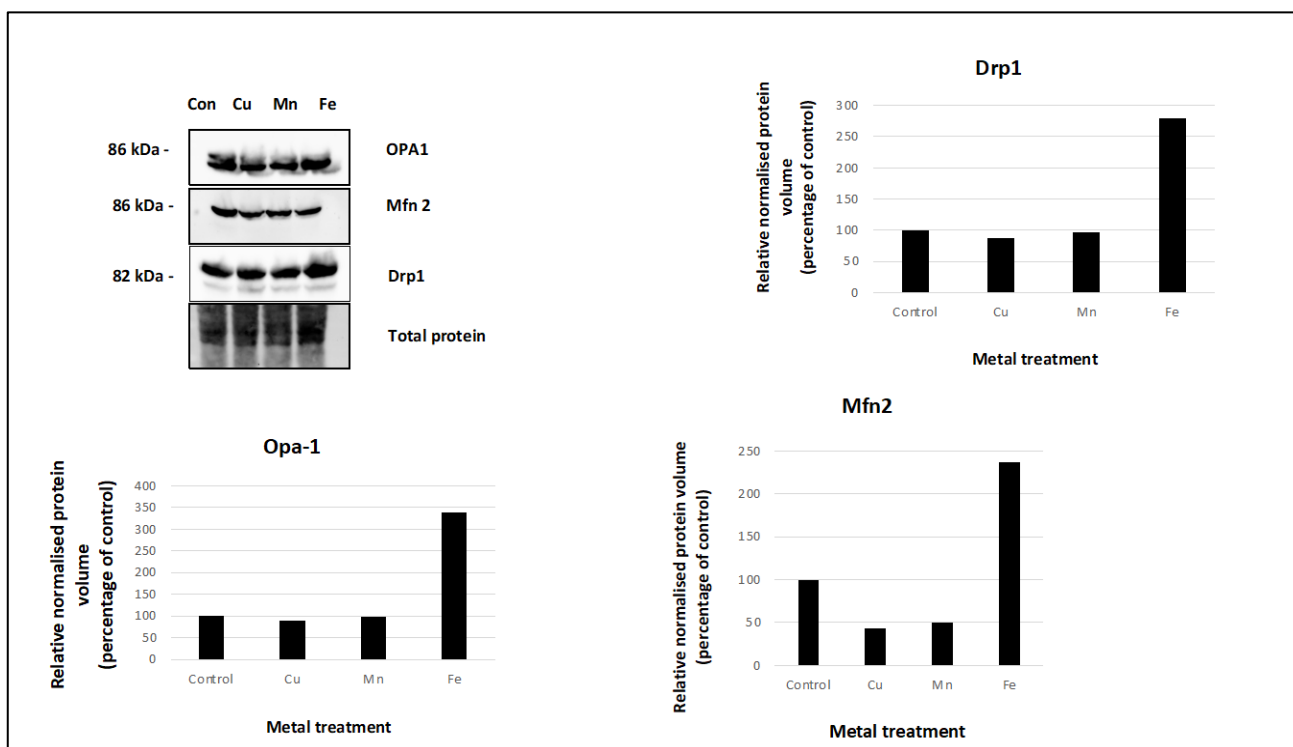


Figure 3.24: Cell viability analysis and cell count after exposure to Fe.



**Figure 3.25: Assessment of mitochondrial fission and fusion proteins after exposure to all metals of interest.**

Optic atrophy-1 (Opa-1) is an essential GTPase that is responsible for the fusion of the inner mitochondrial membrane – its increase could be an indication of up regulated mitochondrial fusion and this could be a stress response mechanism resulting from increased mitochondrial stress. Mfn2 is one of two Fzo Homologues produced by humans and is essential for mito-fusion, furthermore its overexpression can alter mitochondrial morphology. Lower levels of this protein can also lead to decreased mitochondrial fusion which could be the case with Cu and Mn as the protein volumes of these are slightly lower than the control. As in Opa-1, the higher expression of mfn2 re-affirms the notion of an increased mitochondrial fusion in the iron group.

In future, it is recommended that mitochondrial fission and fusion dynamics also be assessed, using live cell imaging and immunofluorescence. In addition, the extent of amyloid beta and alpha synuclein synthesis, when exposed to the above metals also need to be assessed, using western blotting. The information to be obtained from this analyses will with no doubt strengthen the already established data set. A correlative light-and electron microscopy approach can also be implemented, so as to additionally shed light on the molecular identify and ultrastructural context of the neurons when exposed to the respective metals.

## CHAPTER 4: CONCLUSION AND RECOMMENDATIONS

---

### 4.1 CONCLUSIONS

In conclusion, the findings from this study have shown that Cd and Cu have the potential to further exacerbate neurotoxicity in a pre-existing neurodegenerative environment in the context of APP over-expression. Thus, more attention may have to be paid to the preventing the exposure to these specific heavy metals. Moreover, our findings show that surface and river water in the Northern Cape region are a concern, which requires further attention. These findings are of particular importance due to the communities typically exposed to the surface water, either through dermal contact or, given the poor sanitation and water shortage in the region, water ingestion.

The findings from this study can be used to inform the development of guideline values (maximum allowable limits for exposure) for these metals, treatment methods for heavy metal removal in water and as well as inform possible departure for a conversation for other heavy-mining countries to take similar precautions to protect those exposed to heavy metals. In South Africa, this is the first study to assess metal toxicity in the context of neurodegeneration within mining populations. These findings are of particular importance due to the high concentration of copper (mines) and gold mines (mines, of which cadmium is a by-product) found in South Africa. Further action in this context, such as *in vivo* studies, social and corporate activity and prophylactic interventions are recommended for further work.

### 4.2 RECOMMENDATIONS

Taken together, this research highlights that, although municipal water sources in the two respective mining regions are safe and within the regulatory limits, the surface water poses a substantial risk. Moreover, our results reveal that also borehole water may pose a risk, as indicated by the high arsenic levels in one sampling region in the Limpopo area. Indeed, the suspected metals cadmium, copper and manganese appear to have, molecularly, major detrimental effects. Iron, manganese and copper, but also aluminium concentrations are above respective limits in the surface and river waters, which poses risk for the environment and the community in close proximity to these regions.

In many communities, where water had been collected, only a single tap was available for the entire community. This increases the risk for using easily accessible water sources, including surface and river water, for consumption, feeding of life stock or irrigation. The same risk exists when using contaminated borehole water. We therefore suggest further action in this context, such as *in vivo* studies, but also social and corporate activity, to raise awareness and to maximize social corporate investments that protect the environment and communities in the regions assessed.

## REFERENCES

---

1. Abbaspour, N., Hurrell, R. and Kelishadi, R. (2014) 'Review on iron and its importance for human health,' *Journal of research in medical sciences: the official journal of sfahan University of Medical Sciences*, 19(2), pp. 164.
2. Abdul, K.S.M. et al. (2015) 'Arsenic and human health effects: A review,' *Environmental toxicology and pharmacology*, 40(3), pp. 828-846.
3. Anderson, G.J. and Frazer, D.M. (2017) 'Current understanding of iron homeostasis,' *The American journal of clinical nutrition*, 106(6), pp. 1559S-1566S.
4. Angelova, M. et al. (2011) 'Copper in the human organism,' *Trakia Journal of Sciences*, 9(1), pp. 88-98.
5. Archana, M., Yogesh, T.L. and Kumaraswamy, K.L. (2013) 'Various methods available for detection of apoptotic cells – A review,' *Indian journal of cancer*, 50(3), pp. 274.
6. Askham, T.M. and Van der Poll, H.M. (2017) 'Water sustainability of selected mining companies in South Africa,' *Sustainability*, 9(6), pp. 957.
7. Bagheri, S. et al. (2018), 'Role of copper in the onset of Alzheimer's disease compared to other metals,' *Frontiers in aging neuroscience*, (9), pp. 446.
8. Balmuş, I.M. (2017) 'Preliminary data on the interaction between some biometals and oxidative stress status in mild cognitive impairment and Alzheimer's disease patients,' *Oxidative Medicine and Cellular Longevity*.
9. Beaino, W. et al. (2014) 'Roles of Atox1 and p53 in the trafficking of copper-64 tumour cell nuclei: implications for cancer therapy,' *JBIC Journal of Biological Inorganic Chemistry*, 19(3), pp. 427-438.
10. Biel, T.G. et al. (2020) 'Mitochondrial dysfunction generates aggregates that resist lysosomal degradation in human breast cancer cells,' *Cell death & disease*, 11(6), pp.1-15.
11. Bishop, N.A., Lu, T. and Yankner, B.A. (2010) 'Neural mechanisms of ageing and cognitive decline,' *Nature*, 464(7288), pp. 529-535.
12. Brewer, G.J. et al. (2010) 'Copper and ceruloplasmin abnormalities in Alzheimer's disease,' *American Journal of Alzheimer's Disease & Other Dementias*, 25(6), pp. 490-82
13. Carageorgiou, H. et al. (2005) 'Cadmium effects on brain acetylcholinesterase activity and antioxidant status of adult rats: modulation by zinc, calcium and L-cysteine co-administration,' *Basic & clinical pharmacology & toxicology*, 97(5), pp. 320-324.
14. Chen, P. et al. (2015) 'Manganese homeostasis in the nervous system,' *Journal of neurochemistry*, 134(4), pp. 601-610.
15. Darzynkiewicz, Z. (1990) 'Differential staining of DNA and RNA in intact cells and isolated cell nuclei with acridine orange,' *Methods in cell biology*, 33, pp. 285-298.
16. Dlamini, W.W. et al. (2020) 'Manganese exposure, parkinsonian signs, and quality of life in South African mine workers,' *American journal of industrial medicine*, 63(1), pp. 36-43.
17. Dobson, A.W., Erikson, K.M. and Aschner, M. (2004) 'Manganese neurotoxicity,' *ANNALS-NEW YORK ACADEMY OF SCIENCES*, pp. 115-128.
18. Dopp, E. et al. (2010) 'Cellular uptake, subcellular distribution and toxicity of arsenic compounds in methylating and non-methylating cells,' *Environmental Research*, 110(5), pp. 435-442.
19. Dusek, P. et al. (2015) 'The neurotoxicity of iron, copper and manganese in Parkinson's and Wilson's diseases,' *Journal of Trace Elements in Medicine and Biology*, 31, pp. 193-203.
20. du Toit, A. et al. (2018) 'Measuring autophagosome flux. *Autophagy*, 14(6), pp. 1060-1071.
21. Edokpayi, J.N. et al. (2018) 'Evaluation of water quality and human risk assessment due to heavy metals in groundwater around Muledane area of Vhembe District, Limpopo Province, South Africa,' *Chemistry Central Journal*, 12(1), pp. 1-16.
22. Forcella, M. et al. (2020) 'Neuronal specific and non-specific responses to cadmium possibly involved in neurodegeneration: A toxicogenomics study in a human neuronal cell model,' *Neurotoxicology*, 76, pp. 162-173.
23. Galluzzi, L. et al. (2017) 'Molecular definitions of autophagy and related processes,' *The EMBO journal*, 36(13), pp. 1811-1836.
24. Genthe, B. et al. (2018) 'The reach of human health risks associated with metals/metalloids in water and vegetables along a contaminated river catchment: South Africa and Mozambique,' *Chemosphere*, 199, pp. 1-9.
25. Goodman, L.L. (1953) 'Materials and handling and processing – past and present,' *Journal of the Royal Society of Arts*, 101(4905), pp. 672-694.
26. Grasso, G. et al. (2017) 'The double faced role of copper in A $\beta$  homeostasis: a survey on the interrelationship between metal dyshomeostasis, UPS functioning and autophagy in neurodegeneration,' *Coordination Chemistry Reviews*, 347, pp. 1-22.
27. Guilarte, T.R. (2010) 'Manganese and Parkinson's disease: a critical review and new findings,' *Environmental health perspectives*, 118(8), pp. 1071-1080.

28. Hochberg, F. et al. (1996) 'Late motor deficits of Chilean manganese miners: a blinded control study,' *Neurology*, 47(3), pp. 788-795.
29. Hung, Y.H., Bush, A.I. and Cherny, R.A. (2010) 'Copper in the brain and Alzheimer's disease,' *JBIC Journal of Biological Inorganic Chemistry*, 15(1), pp. 61-76.
30. Hsu, H.W., Bondy, S.C. and Kitazawa, M. (2018) 'Environmental and dietary exposure to copper and its cellular mechanisms linking to Alzheimer's disease,' *Toxicological sciences*, 163(2), pp. 338-345.
31. Issa, A.R. et al. (2018) 'The lysosomal membrane protein LAMP2A promotes autophagic flux and prevents SNCA-induced Parkinson disease-like symptoms in the Drosophila brain,' *Autophagy*, 14(11), pp. 1898-1910.
- Kerr, J.F., Wyllie, A.H. and Currie, A.R. (1972) 'Apoptosis: a basic biological phenomenon with wideranging implications in tissue kinetics,' *British journal of cancer*, 26(4), pp. 239-257.
32. Khan, I.U. et al. (2020) 'Functional characterization of a new metallochaperone for reducing cadmium concentration in rice crop,' *Journal of Cleaner Production*, 272, pp.123152.
33. Kocaturk, N. and Gozuacik, D. (2018) 'Crosstalk between mammalian autophagy and the ubiquitin-proteasome system,' *Frontiers in cell and developmental biology*, 6, pp.128.
34. Kurz, T. et al. (2008) 'Lysosomes in iron metabolism, ageing and apoptosis,' *Histochemistry and cell biology*, 129(4), pp. 389-406.
35. Lanyon, R. (1997) 'Arsenic dispersion associated with the Barbrook gold mine in the Mpumalanga Province of South Africa,' (Master's thesis, University of Cape Town).
36. Levine, B. and Kroemer, G. (2008) 'Autophagy in the pathogenesis of disease,' *Cell*, 132(1), pp. 27-42.
37. Lin, Y., Epstein, D.L. and Liton, P.B. (2010) 'Intralysosomal iron induces lysosomal membrane permeabilization and cathepsin D-mediated cell death in trabecular meshwork cells exposed to oxidative stress,' *Investigative ophthalmology & visual science*, 51(12), pp. 6483-6495.
38. Lucchini, R. et al. (1999) 'Long-term exposure to "low levels" of manganese oxides and neurofunctional changes in ferroalloy workers,' *Neurotoxicology*, 20(2-3), pp. 287-297.
39. Lumkwana, D. et al. (2017) 'Autophagic flux control in neurodegeneration: Progress and precision targeting—Where do we stand?' *Progress in neurobiology*, 153, pp. 64-85.
40. Lutsenko, S. (2010) 'Human copper homeostasis: a network of interconnected pathways,' *Current opinion in chemical biology*, 14(2), pp. 211-217.
41. Madsen, E. and Gitlin, J.D. (2007) 'Copper and iron disorders of the brain,' *Annu. Rev. Neurosci.*, 30, pp. 317-337.
42. Malan, M. et al. (2015) 'Heavy metals in the irrigation water, soils and vegetables in the Philippi horticultural area in the Western Cape Province of South Africa,' *Environmental monitoring and assessment*, 187(1), pp. 1-8.
43. Martins, A.C. et al. (2019) 'New insights on the role of manganese in Alzheimer's disease and Parkinson's disease.,' *International journal of environmental research and public health*, 16(19), pp. 3546.
44. Mativenga, P.T. and Marnewick, A. (2018) 'Water quality in a mining and water-stressed region,' *Journal of cleaner production*, 171, pp. 446-456.
45. Mergler, D. et al. (1999) 'Manganese neurotoxicity, a continuum of dysfunction: results from a community based study,' *Neurotoxicology*, 20(2-3), pp. 327-342.
46. Messner, B. et al. (2012) 'Cadmium activates a programmed, lysosomal membrane permeabilization-dependent necrosis pathway,' *Toxicology letters*, 212(3), pp. 268-275.
47. Minami, A. et al. (2001) 'Cadmium toxicity in synaptic neurotransmission in the brain,' *Brain research*, 894(2), pp. 336-339.
48. Myers, J.E. et al. (2003) 'Nervous system effects of occupational manganese exposure on South African manganese mineworkers,' *Neurotoxicology*, 24(4-5), pp. 649-656.
49. Ndayisaba, A., Kaindlstorfer, C. and Wenning, G.K. (2019) 'Iron in neurodegeneration – cause or consequence?' *Frontiers in neuroscience*, 13, pp. 180.85
50. Nixon, R.A. and Yang, D.S. (2011) 'Autophagy failure in Alzheimer's disease – locating the primary defect,' *Neurobiology of disease*, 43(1), pp. 38-45.
51. Ntsapi, C.M. and Loos, B. (2021) 'Neurons die with heightened but functional macro- and chaperone mediated autophagy upon increased amyloid- $\beta$  induced toxicity with region-specific protection in prolonged intermittent fasting,' *Experimental Cell Research*, 408(2), pp. 112840.
52. Olobatoke, R.Y. and Mathuthu, M. (2015) 'Radionuclide exposure in animals and the public health implications,' *Turkish Journal of Veterinary & Animal Sciences*, 39(4), pp.381-388.
53. Opazo, C.M., Greenough, M.A. and Bush, A.I. (2014) 'Copper: from neurotransmission to neuroproteostasis,' *Frontiers in aging neuroscience*, 6, pp. 143.
54. Pattayil, L. and Balakrishnan-Saraswathi, H.T. (2019) 'In vitro evaluation of apoptotic induction of butyric acid derivatives in colorectal carcinoma cells,' *Anticancer research*, 39(7), pp. 3795-3801.
55. Pellacani, C. and Costa, L.G. (2018) 'Role of autophagy in environmental neurotoxicity,' *Environmental Pollution*, 235, pp. 791-805.
56. Pi, H. et al. (2017) 'Enhancing lysosomal biogenesis and autophagic flux by activating the transcription factor EB protects against cadmium-induced neurotoxicity,' *Scientific reports*, 7(1), pp. 1-14.

57. Pohanka, M. (2019) 'Copper and copper nanoparticles toxicity and their impact on basic functions in the body,' *Bratisl. Lek. Listy*, 120(6), pp. 397-409.
58. Polykretis, P. et al. (2019) 'Cadmium effects on superoxide dismutase 1 in human cells revealed by NMR,' *Redox biology*, 21, pp. 101102.
59. Prakash, C., Soni, M. and Kumar, V. (2016) 'Mitochondrial oxidative stress and dysfunction in arsenic neurotoxicity: a review,' *Journal of Applied Toxicology*, 36(2), pp. 179-188.
60. Rani, A., Kumar, A., Lal, A. and Pant, M. (2014) 'Cellular mechanisms of cadmium-induced toxicity: a review,' *International journal of environmental health research*, 24(4), pp. 378-399.
61. Razak, M.R. et al. (2021) 'Accumulation and risk assessment of heavy metals employing species sensitivity distributions in Linggi River, Negeri Sembilan, Malaysia,' *Ecotoxicology and environmental safety*, 211, pp. 111905.
62. Rubinsztein, D.C., Codogno, P. and Levine, B. (2012) 'Autophagy modulation as a potential therapeutic target for diverse diseases,' *Nature reviews Drug discovery*, 11(9), pp. 709-730.
63. Scimeca, M. et al. (2018) 'Energy Dispersive X-ray (EDX) microanalysis: A powerful tool in biomedical research and diagnosis,' *European journal of histochemistry: EJH*, 62(1).
64. Sedibe, M. et al. (2017) 'South African mine effluents: Heavy metal pollution and impact on the ecosystem.'
65. Singh, R. et al. (2010) 'Biosorption optimization of lead (II), cadmium (II) and copper (II) using response surface methodology and applicability in isotherms and thermodynamics modelling,' *Journal of hazardous materials*, 174(1-3), pp. 623-634.
66. Snyder, H. and Wolozin, B. (2004) 'Pathological proteins in Parkinson's disease,' *Journal of Molecular Neuroscience*, 24(3), pp. 425-442.
67. South African National Standards for drinking water (2015). Retrieved from [https://web.mwa.co.th/download/prd01/iDW\\_standard/South\\_African\\_Water\\_Standard\\_SANS\\_241-2015.pdf](https://web.mwa.co.th/download/prd01/iDW_standard/South_African_Water_Standard_SANS_241-2015.pdf) [Accessed on 22/03/2021].
68. Squitti, R. et al. (2002) 'Elevation of serum copper levels in Alzheimer's disease,' *Neurology*, 59(8), pp. 1153-1161.
69. Sun, A.Y. et al. (2010) 'Resveratrol as a therapeutic agent for neurodegenerative diseases,' *Molecular neurobiology*, 41(2), pp. 375-383.
70. Suzuki, H. et al. (1983) 'Role of brain lysosomes in the development of manganese toxicity in mice,' *Toxicology and applied pharmacology*, 71(3), pp. 422-429.
71. Tamás, M.J. et al. (2014) 'Heavy metals and metalloids as a cause for protein misfolding and aggregation,' *Biomolecules*, 4(1), pp. 252-267.
72. Thakur, M. et al. (2021) 'Molecular Mechanism of Arsenic-Induced Neurotoxicity including Neuronal Dysfunctions,' *International Journal of Molecular Sciences*, 22(18), pp. 10077.
73. Thinakaran, G. et al. (1996) 'Metabolism of the "Swedish" amyloid precursor protein variant in neuro2a (N2a) cells: evidence that cleavage at the "β-secretase" site occurs in the Golgi apparatus,' *Journal of Biological Chemistry*, 271(16), pp. 9390-9397.
74. Thomas, G. et al. (2021) 'Regional brain iron and gene expression provide insights into neurodegeneration in Parkinson's disease,' *Brain*.87
75. Tyler, C.R. and Allan, A.M. (2014) 'The effects of arsenic exposure on neurological and cognitive dysfunction in human and rodent studies: a review,' *Current environmental health reports*, 1(2), pp. 132-147.
76. United States Environmental Protection Agency, 'Guidelines for water reuse' (2004). Retrieved from
77. [https://sswm.info/sites/default/files/reference\\_attachments/30006MKD.pdf](https://sswm.info/sites/default/files/reference_attachments/30006MKD.pdf). [Accessed on 03/04/2022].
78. Upreti, R.K., Shrivastava, R. and Chaturvedi, U.C. (2004) 'Gut microflora & toxic metals: chromium as a model,' *Indian Journal of Medical Research*, 119, pp. 49-59.
79. Vahter, M. (2008) 'Health effects of early life exposure to arsenic,' *Basic & clinical pharmacology & toxicology*, 102(2), pp. 204-211.
80. Vergilio, C.D.S. and De Melo, E.J.T. (2013) 'Autophagy, apoptosis and organelle features during cell exposure to cadmium,' *Biocell*, 37(2), pp. 45.
81. Wan, F. et al. (2020) 'Long-term exposure to copper induces autophagy and apoptosis through oxidative stress in rat kidneys,' *Ecotoxicology and Environmental Safety*, 190, pp. 110158.
82. Water Access in South Africa (2017). Retrieved from <http://12.000.scripts.mit.edu/mission2017/case-studies/water-access-in-south-africa/#:~:text=Currently%2C%2019%20percent%20of%20the,water%20access%20eith%20%5B1%5D>. [Accessed on 14/03/2021].
83. Weber, R.A. et al. (2020) 'Maintaining iron homeostasis is the key role of lysosomal acidity for cell proliferation,' *Molecular cell*, 77(3), pp. 645-655. World Health Organisation guidelines for drinking water quality (2011). Retrieved from Wu, J.S. et al. (2013) 'Imaging and elemental mapping of biological specimens with a dual-EDS dedicated scanning transmission electron microscope,' *Ultramicroscopy*, 128, pp. 24-31.

84. Wortmann, M. (2012) 'Dementia: a global health priority-highlights from an ADI and World Health Organization report,' *Alzheimer's research & therapy*, 4(5), pp. 1-3. [https://apps.who.int/iris/bitstream/handle/10665/44584/9789241548151\\_eng.pdf](https://apps.who.int/iris/bitstream/handle/10665/44584/9789241548151_eng.pdf). [Accessed on 14/03/2021].
  85. Wu, Q. et al. (2020) 'Overexpression of p62 induces autophagy and promotes proliferation, migration and invasion of nasopharyngeal carcinoma cells through promoting ERK signaling pathway,' *Current Cancer Drug Targets*, 20(8), pp. 624-637.
  86. Xu, C. et al. (2021) 'Cadmium Impairs Autophagy Leading to Apoptosis by Ca<sup>2+</sup>- Dependent Activation of JNK Signaling Pathway in Neuronal Cells,' *Neurochemical Research*, 46(8), pp. 2033-2045.
  87. Yan, D.Y. and Xu, B. (2020) 'The role of autophagy in manganese-induced neurotoxicity,' *Frontiers in Neuroscience*, 14, pp. 574750.
  88. Yin, L.M. et al. (2013) 'Long term and standard incubations of WST-1 reagent reflect the same inhibitory trend of cell viability in rat airway smooth muscle cells,' *International Journal of Medical Sciences*, 10(1), pp. 68.
  89. Yokel, R.A. (2006) 'Blood-brain barrier flux of aluminum, manganese, iron and other metals suspected to contribute to metal-induced neurodegeneration,' *Journal of Alzheimer's Disease*, 10(2-3), pp. 223-253.
  90. Yuan, J. et al. (2021) 'Cadmium induces endosomal/lysosomal enlargement and blocks autophagy flux in rat hepatocytes by damaging microtubules,' *Ecotoxicology and Environmental Safety*, 228, pp. 112993.
  91. Zeng, X. et al. (2020) 'Neurodegenerative diseases among miners in Ontario, Canada, using a linked cohort,' *Occupational and Environmental Medicine*.
  92. Zhang, Z. et al. (2020) 'Dysregulation of TFEB contributes to manganese-induced autophagic failure and mitochondrial dysfunction in astrocytes,' *Autophagy*, 16(8), pp.1506-1523.
  93. Zheng, W., Aschner, M. and Ghersi-Egea, J.F. (2003) 'Brain barrier systems: a new frontier in metal neurotoxicological research,' *Toxicology and applied pharmacology*, 192(1), pp. 1-11.
  94. Zheng, W. and Monnot, A.D. (2012) 'Regulation of brain iron and copper homeostasis by brain barrier systems: implication in neurodegenerative diseases,' *Pharmacology & therapeutics*, 133(2), pp. 177-188.
  95. Zhu, Y.G. et al. (2008) 'High percentage inorganic arsenic content of mining impacted and nonimpacted Chinese rice,' *Environmental science & technology*, 42(13), pp. 5008-5013.
  96. Zhu, X.X. et al. (2014) 'Sodium arsenite induces ROS-dependent autophagic cell death in pancreatic  $\beta$ -cells,' *Food and chemical toxicology*, 70, pp. 144-150.
-